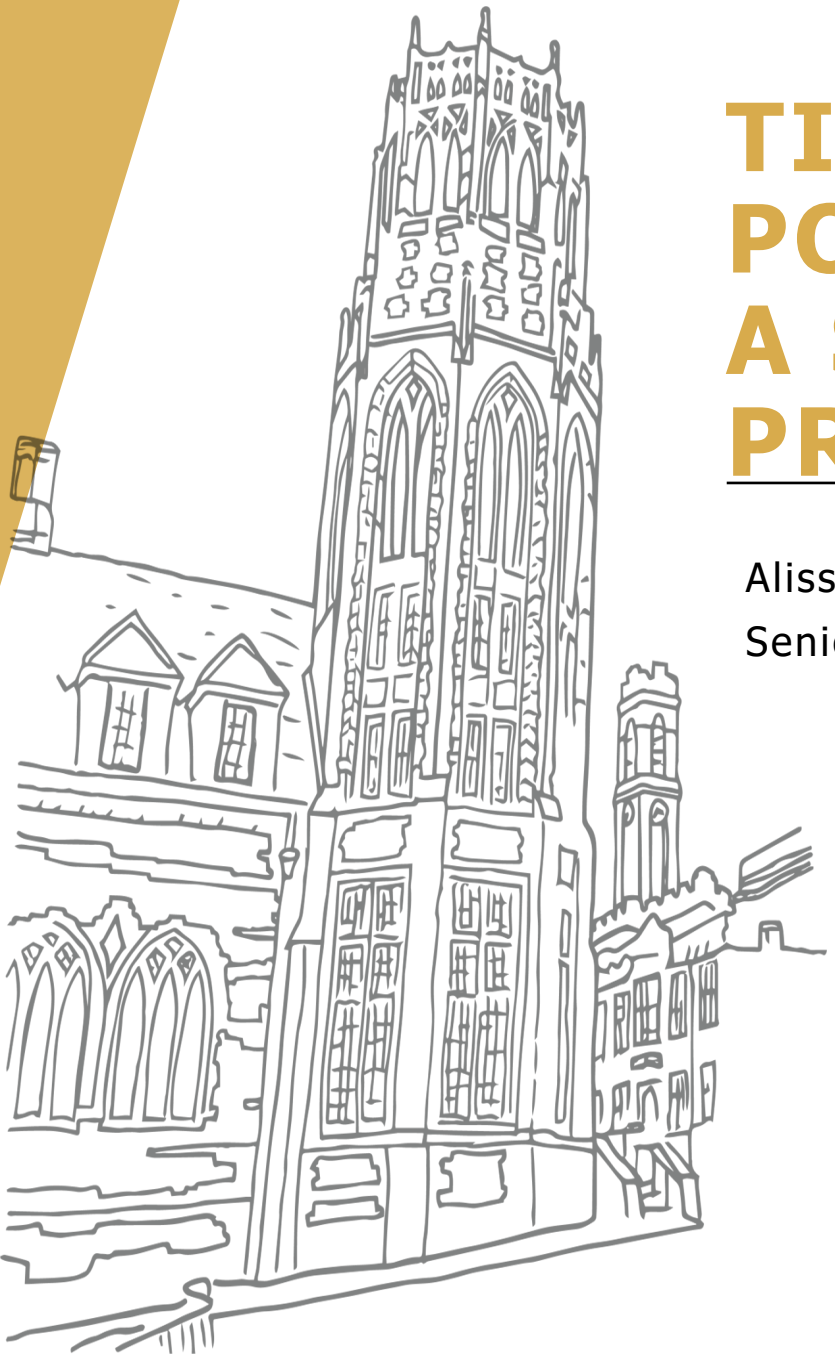

TIPS ON MAKING A POSTER AND HAVING A SUCCESSFUL PRESENTATION

Alissa Hare

Senior Lecturer in Chemistry

VANDERBILT UNIVERSITY

Poster Sessions – presenting basics

- Most poster sessions are set up in large rooms with rows of posters and presenters
- People will mill around, some people will want to engage you and hear about your work and some will walk right by – but don't be offended! There is only a limited amount of time for the audience to hear information and they might pick topics that most interest them

VANDERBILT UNIVERSITY

Photo source: Ecological Society of America meeting 2019 in Louisville KY,

Presenting your work to others

- During the session, if you see someone pausing to look at your poster, the thing to ask them is "would you like me to walk you through my poster?"
- Most people are expecting a 5-minute explanation of your poster and work – **that means you can practice!**
- Going through your poster before you get to the session ensures that you have a smooth experience!

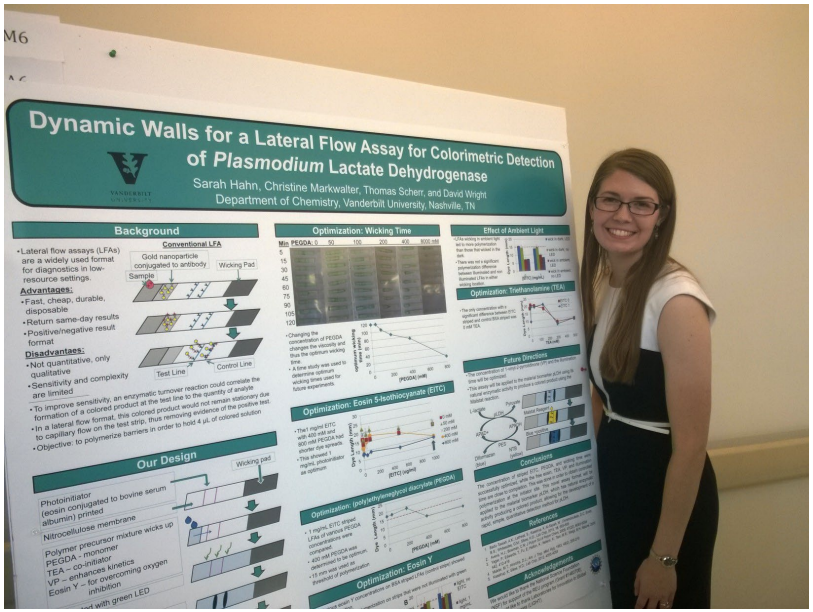

Presenting your poster can lead to important feedback!

- New experiments to run
- New research avenues
- Maybe even new collaborations!

VANDERBILT UNIVERSITY

Preparing the poster as a record

- Forces you to sit down and analyze your data
  - as well as organize your results for the future
- Generates a record of your work for future students and researchers in your lab
- At the end of the summer, it will act as one of the records of your research

Poster Basics – General Template

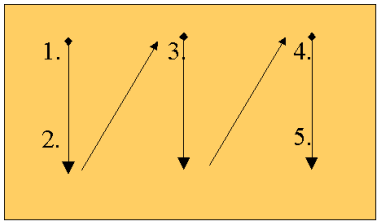

The Role of Calcium In the Function of Calprotectin

Kristen Huseman [1] Eric P. Skaar [2] , and Walter J. Chazin [1]

1 Departments of Biochemistry and Chemistry, Center for Structural Biology, Vanderbilt University, Nashville, TN 37235

2 Department of Pathology, Microbiology, and Immunology, Vanderbilt University Medical Center, Nashville, TN 37235

1. Introduction

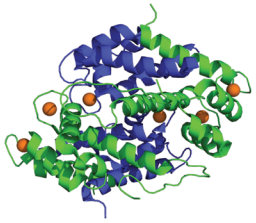

- Calprotectin (S100A8/S100A9, CP) is an EF-hand calcium binding protein that plays a pivotal role in the innate immune response.
- CP functions in nutritional immunity by sequestering transition metals vital to pathogens' survival.
- Calcium binding induces conformational changes, promotes tetramerization, and increases CP's affinity for transition metals.

2. Calcium Binds to CP In EF Hand Motifs

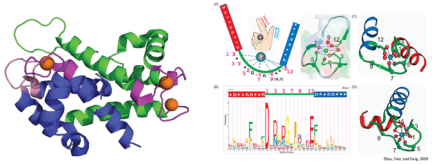

- S100A8 E70Q/S100A9 WT (A8CaKO)
- S100A8 WT/S100A9 E60Q/E78Q (A9CaKO)

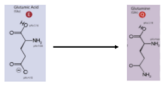

- Wildtype CP contains three canonical EF-hand domains which are conserved domains with a twelve amino acid consensus sequence surrounded by two alpha helices.
- In CP, the ionic interaction between calcium and the negatively charged glutamic acid in the twelfth position of the consensus sequence is vital for the coordination of calcium in the binding site.
- In order to better understand the role of the interaction of calcium with each subunit in the function of CP two CP variants were designed in which only one subunit had lost the ability to bind to calcium.

3. Calcium Binding Is Necessary to Form Tetramers

Circular Dichroism

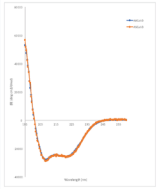

- Both variants had the same amount of helical content.

Dynamic Light Scattering

A8CaKO/A9WT-EDTA

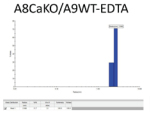

A8CaKO/A9WT-4eqCa

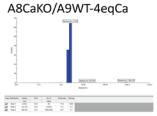

A8WT/A9CaKO-EDTA

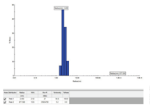

A8WT/A9CaKO-4eqCa

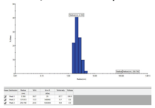

- Even in an excess of calcium, the variants remain dimers and do not tetramerize.
- DLS suggests higher order aggregation of A9CaKO

4. Calcium Binding Induces Conformational Changes

A8CaKO/A9WT

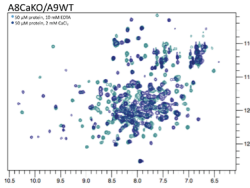

- The large amount of chemical shift perturbations with the addition of calcium is indicative of conformational change on CP.

A8WT/A9CaKO

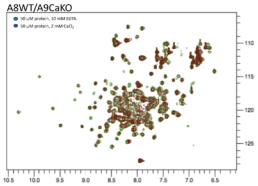

- The decrease in intensity with the addition of calcium is indicative of aggregation which is consistent with DLS data.

5. The Inability to Bind Calcium Suppresses Nutritional Immunity and the Ability to Chelate Zinc

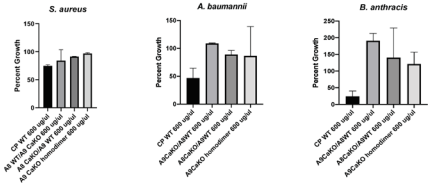

- Percentage of growth determined by optical density at 600 nm at hour 20 of growth
- Both A8CaKO and A9CaKO have decreased bactericidal effects compared to the WT CP.

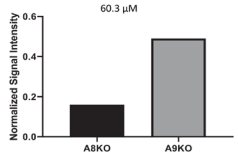

- A8CaKO has a higher affinity for zinc than A9CaKO

6. Conclusions and Future Directions

- Calcium binding is vital to the function of calprotectin.
- Crystallization screening is ongoing to find conditions for high resolution crystal diffraction to determine the structural differences between these two variants responsible for the functional differences.
- Competition-based fluorescence assays should be used to determine the zinc affinity of A8CaKO and A9CaKO and to compare it to that of WT.
- A CP variant will be made in which both subunits have lost the ability to bind to calcium to further test the role of calcium and it's interaction with calprotectin in the immune response.

7. Acknowledgments

We acknowledge the assistance of Simone Harrison in CP expression, Swati Balakrishnan in NMR data collection and analysis, and Aslin Rodriguez-Nassif and Andy Weiss for their training and guidance. We acknowledge NSF REU 1460706 for their financial support for this summer internship.

VANDERBILT UNIVERSITY

Poster Basics – General Template

Sensitivity of Mitochondrial Cytochrome P450s to Adrenodoxin Variation

Margo Goldfarb[1], Ian Barckhausen[2], Stella A. Child[2], Michael J. Reddish[2], F. Peter Guengerich[2]

[1]Department of Chemistry, Kenyon College, Gambier, OH

[2]Department of Biochemistry, Vanderbilt University, Nashville, TN

Introduction

Mitochondrial cytochromes P450 (P450s) are integral to the metabolism of steroids and vitamin D in humans. Their catalytic function relies on the formation of complexes with reduction partners, adrenodoxin (Adx) and NADPH-adrenodoxin reductase (Adr), for electron transfer. The current body of knowledge regarding the thermodynamic potential for interaction is lacking. Previous work suggests that the complex formation relies on contributions from multiple recognition sites that could vary among isoforms from different species. Additionally, the ratio of Adx to P450s may play an important role regulating enzyme activity. Towards the goal of better understanding the the sensitivity of human P450s to both native and non-native Adx isoforms, we aim to functionally characterize these multi-enzyme complexes at varying Adx concentrations for each isoform. Here, we report the steady-state enzyme kinetics of human P450s 11B2 and 27A1 and human and bovine Adx isoforms.

Mitochondrial P450 Reductase System

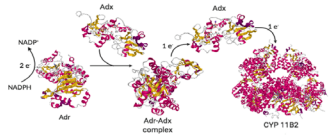

Scheme 1. The electron transport system whereby mitochondrial P450s receive electrons for the catalysis of monooxygenation reactions from NADPH via Adr and Adx. (P450s and the two components of the reductase system, while shown in equimolar amounts, this is not supported by experimental data.)

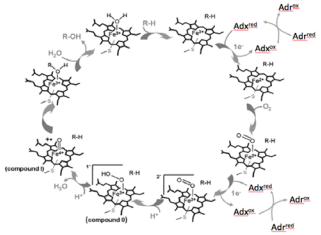

Scheme 2. General catalytic cycle for monooxygenation of RH by mitochondrial P450s.[1] Electron transfer from Adr through Adx occurs in two separate steps of the catalytic cycle.

Recombinant Expression and Purification

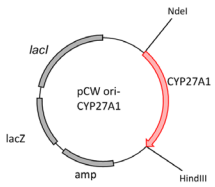

Figure 1. pCW vector used for recombinant expression of mitochondrial P450, 27A1, in *Escherichia coli*. The plasmid includes an C-terminal histidine tag and an ampicillin resistance gene. The coding sequence was modified to facilitate high-level recombinant enzyme expression in *E. coli*.

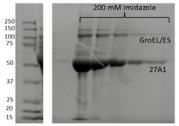

Figure 2. SDS-PAGE analysis of the immobilized metal affinity chromatography (IMAC) fractions for cytochrome P450, 27A1 (kDa) target protein. Fractions with the highest abundance were collected after step-elution with increasing concentrations of imidazole.

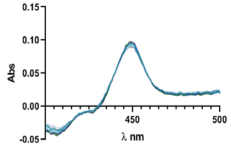

Figure 3. CO-reduced difference spectrum of dialyzed 27A1 absorbs predominantly at 450 nm. Using ε_{450}= 90 mM^{-1}·cm^{-1}, a concentration of correctly folded protein with heme incorporation was determined to be 8.8 µM.

Steady-State P450 Kinetics

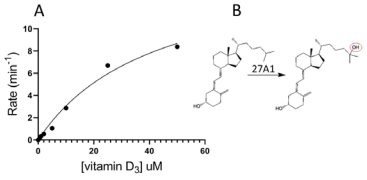

Figure 4. Michaelis–Menten plot for the metabolism of vitamin D_3 by CYP27A1 (A). Incubations were carried out with 0.2 µM CYP27A1 supported by Adr:Adx for 10 min. The plotted lines represent a non-linear regression to the data. The hydroxylation of vitamin D_3 to 25-hydroxy vitamin D_3 catalyzed by CYP27A1 is shown as well (B).

Adrenodoxin Binding Affinity

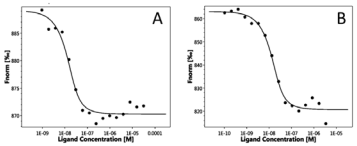

Figure 5. Microscale thermophoresis (MST) analysis of redox partners, Adr (A) and CYP11B2 (B) reveal K_d values for Adx to be 4.6 nM and 4.5 nM, respectively. The equilibrium binding curves are depicted as thick lines.

Adrenodoxin-dependent Kinetics

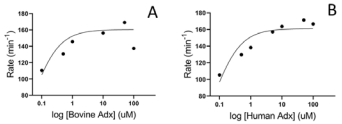

Figure 6. Dependence of CYP11B2 on the concentration of bovine (A) and human (B) adrenodoxin. Preliminary data indicates that the highest activity is reached with approximately 1-5 µM Adx and that there is little to no difference between isoforms.

Conclusions and Directions

- CYP27A1 was recombinantly expressed and purified using IMAC.
- CYP27A1 showed activity towards vitamin D_3 comparable to previous literature values.[2]
- We have demonstrated a near 10,000-fold incongruence in the thermodynamic interaction and the reactivity between Adx and CYP11B2.
- CYP11B2 is sensitive to the concentration of Adx, but not the species of Adx.
- Future work will aim to characterize the sensitivity of additional mitochondrial P450s to Adx variation

References

1. Munro, A. W., Girvan, H. M., & McLean, K. J. (2007). Variations on a (t) heme—novel mechanisms, redox partners and catalytic functions in the cytochrome P450 superfamily. *Natural product reports*, *24*(3), 585-609.
2. Sawada, N., Sakaki, T., Ohta, M., & Inouye, K. (2000). Metabolism of vitamin D3 by human CYP27A1. *Biochemical and biophysical research communications*, *273*(3), 977-984.

Acknowledgments

I would like to thank the contributing authors for their expert guidance on this project. Additionally, I would like to thank Ian Barckhausen for providing the MST data. This work was conducted as part of the 2019 Research Experience for Undergraduates (REU) in Chemical Biology and supported by the National Science Foundation (NSF REU 1460706) and the National Institutes of Health (NIH grant GM118122).

Getting Started

1. Try to tell the story through graphics!
   Which plots, graphs and other images will help you get the story across?

2. Make an outline first

Background
- Frame the research problem
- Why should the listener care
- Is there a graph or chart that can fit here?

Methods
- Explain how you are doing the research
- Define methods and don't assume your listener understands how the experiments are run

Results
- Focus on 3-4 main results
- Use graphics to support your claims = charts, graphs, pictures

Key Takeaways
- What have you concluded from the experiments above?
- What is next?

Making the Poster

- Then sketch out on paper and pencil and rough layout
- Include example title headings, sketches of charts and start filling in bullet points

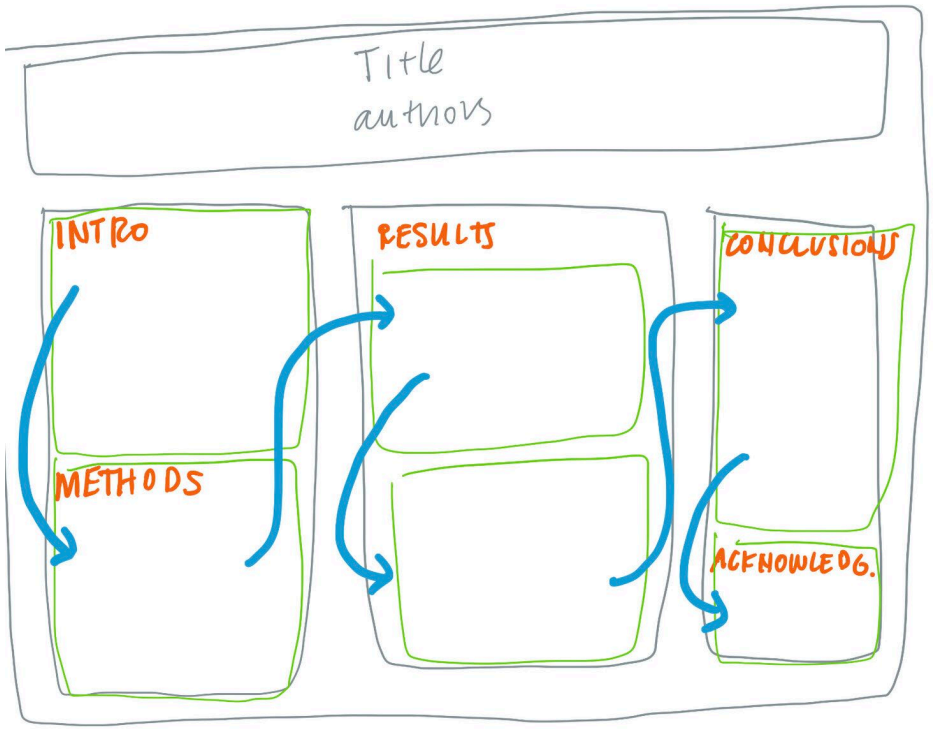

How to make a scientific poster — Callie R. Chappell (calliechappell.com)

Making the Poster

PowerPoint

- Easy to use
- Somewhat Inflexible
- Designed for overhead projection
- But colors can be deceiving

Adobe Illustrator

- Excellent
- More difficult to learn
- What you see is what you get
- Others: Canvas, Publish-It, Corel Draw, InDesign

VANDERBILT UNIVERSITY

Making the Poster

- Then use this sketch to guide your poster file
- Borrow a template from a grad student as a starting point!

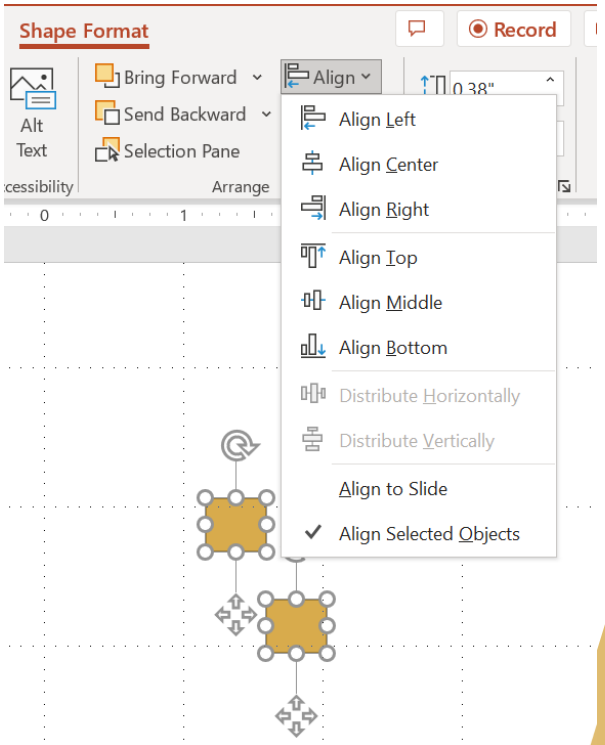

- Resizing, aligning and other formatting issues take time – regardless of the program you are using
- So once you have a layout sketch, get started!

Making the Poster

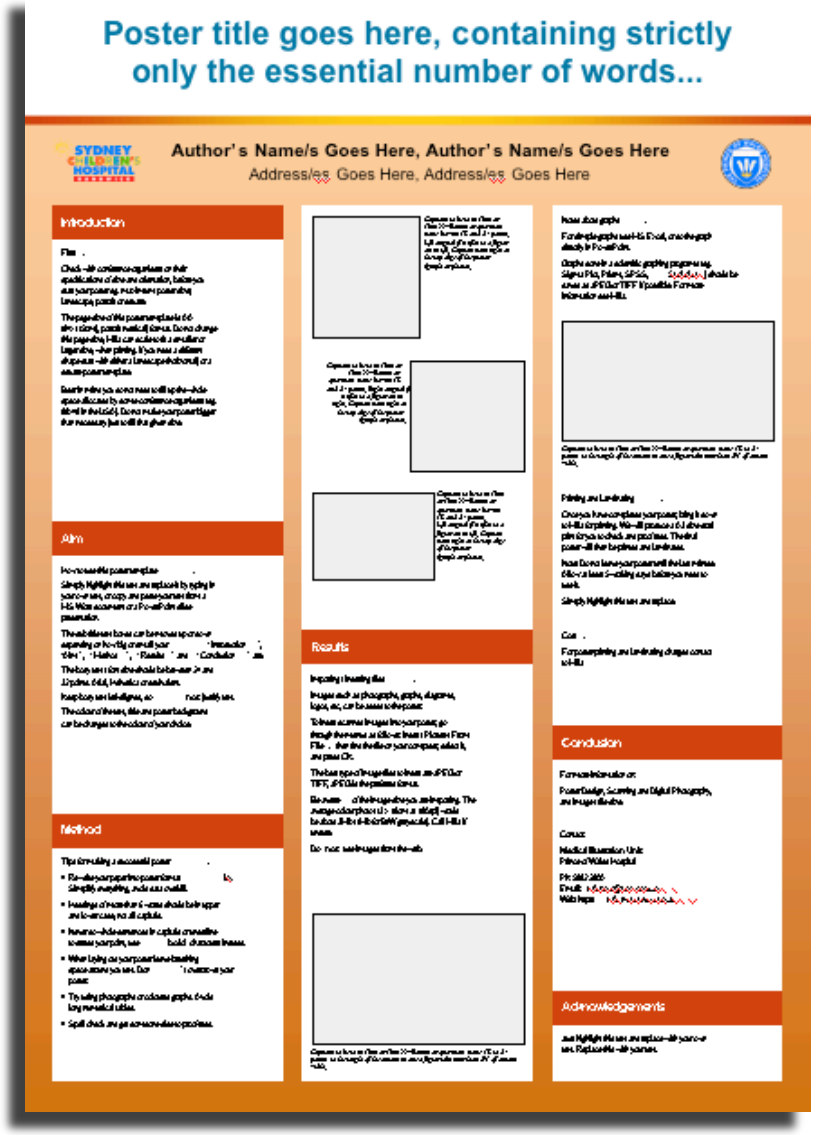

- Leave breathing space around your text – don't fill every bit!
- Serif font works great for the small text
- Same size and style in all blocks of copy

VANDERBILT UNIVERSITY

Making the Poster

Title: **85 point**

Authors: **56pt**

Sub-headings: **36pt**

Body text: **24pt**

Captions: **18pt**

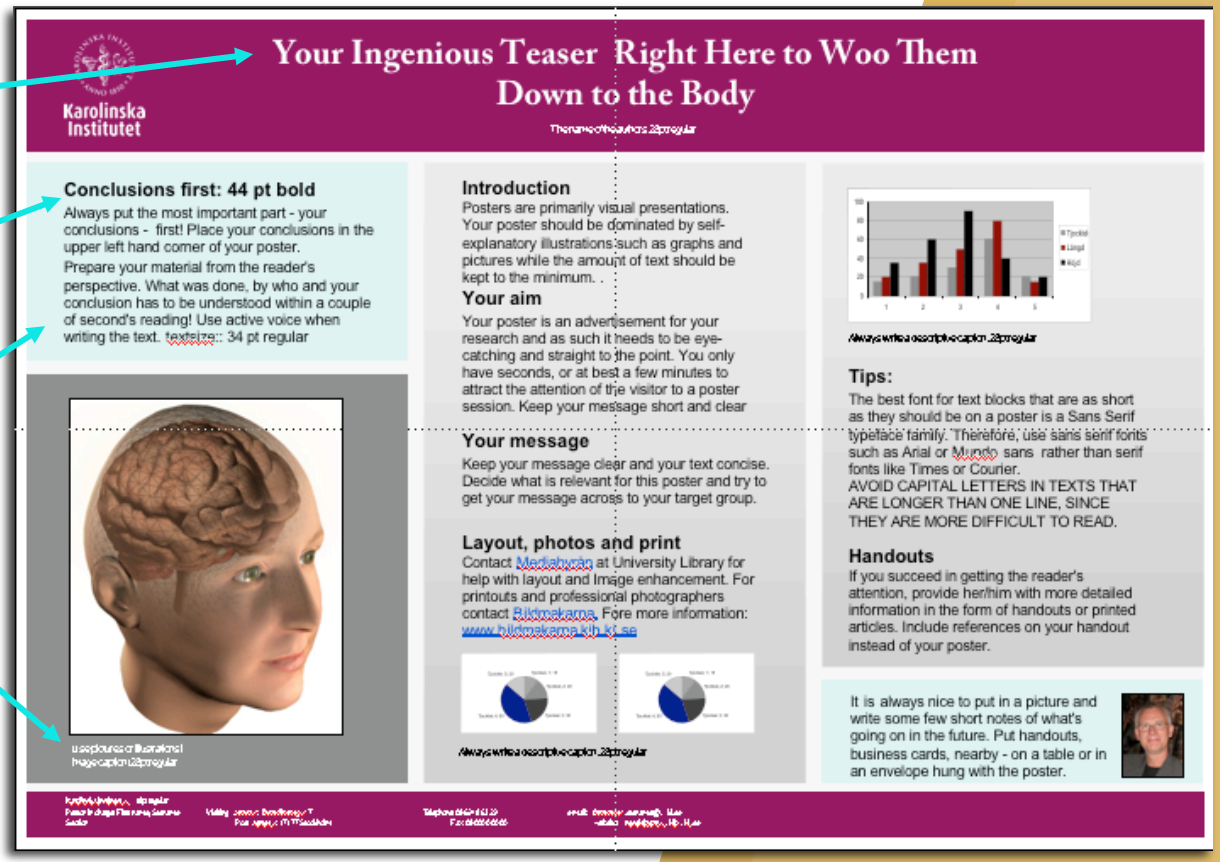

VANDERBILT UNIVERSITY

Keep the Graphics Easy to Read

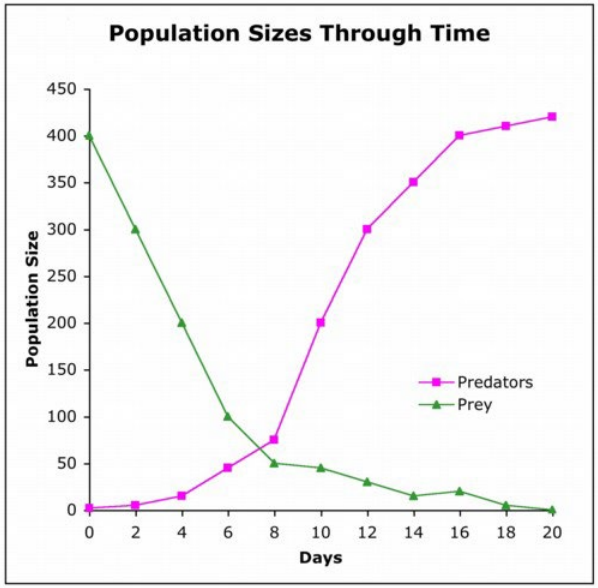

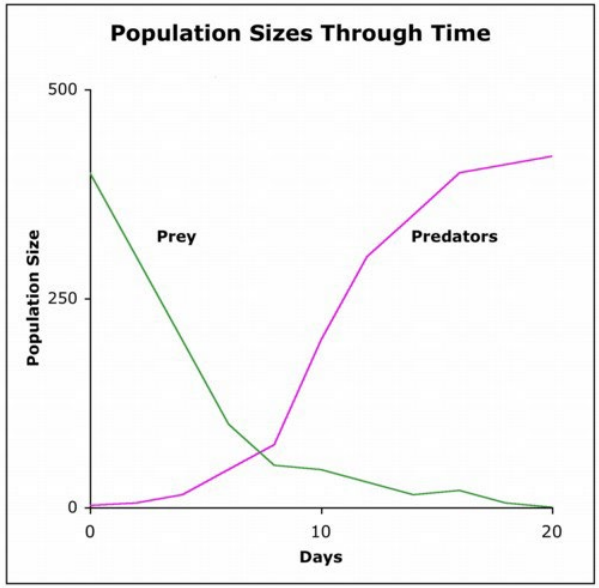

The graphics do not have to be formatted for a journal article – focus on making them easy to read and understand

Keep the Graphics Easy to Read

Line art is best displayed as a "png"

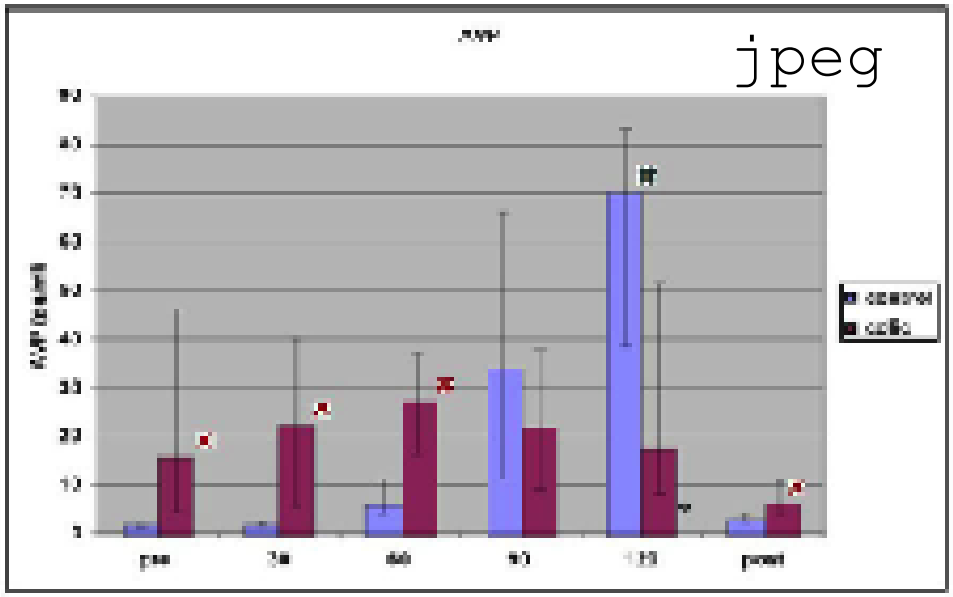

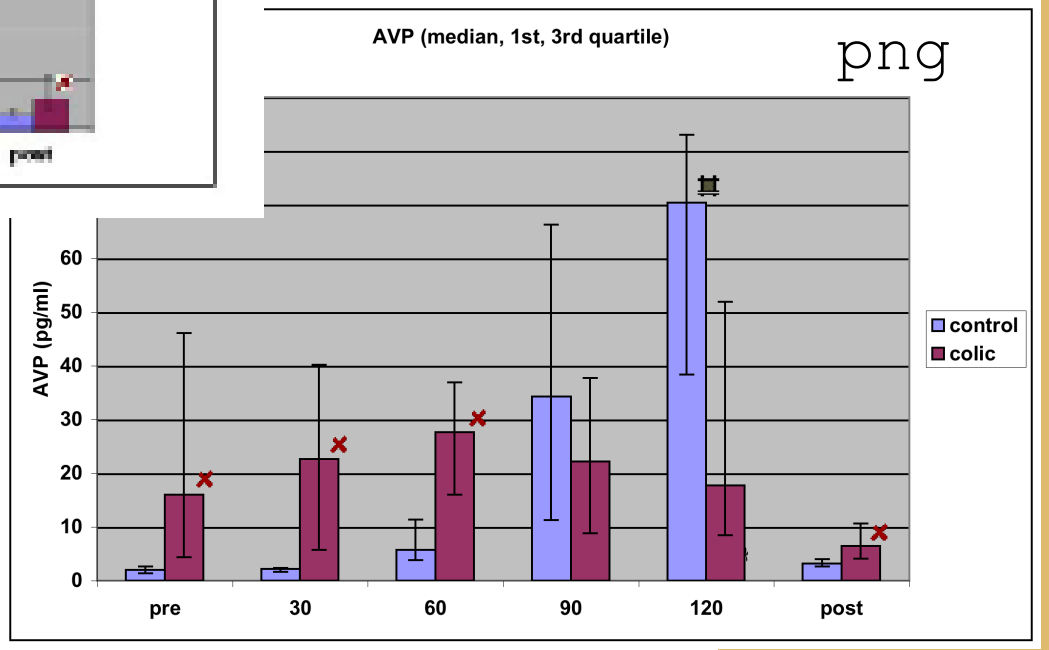

Editing your poster

- Once you've got a draft of your poster, ask yourself if there is any thing that makes the poster look too busy
- Remove fancy font, extra backgrounds and edit colors so you have a cohesive color palette
- Send it to your lab mates for comments and edits – they know your research well and will be able to help smooth over any problems

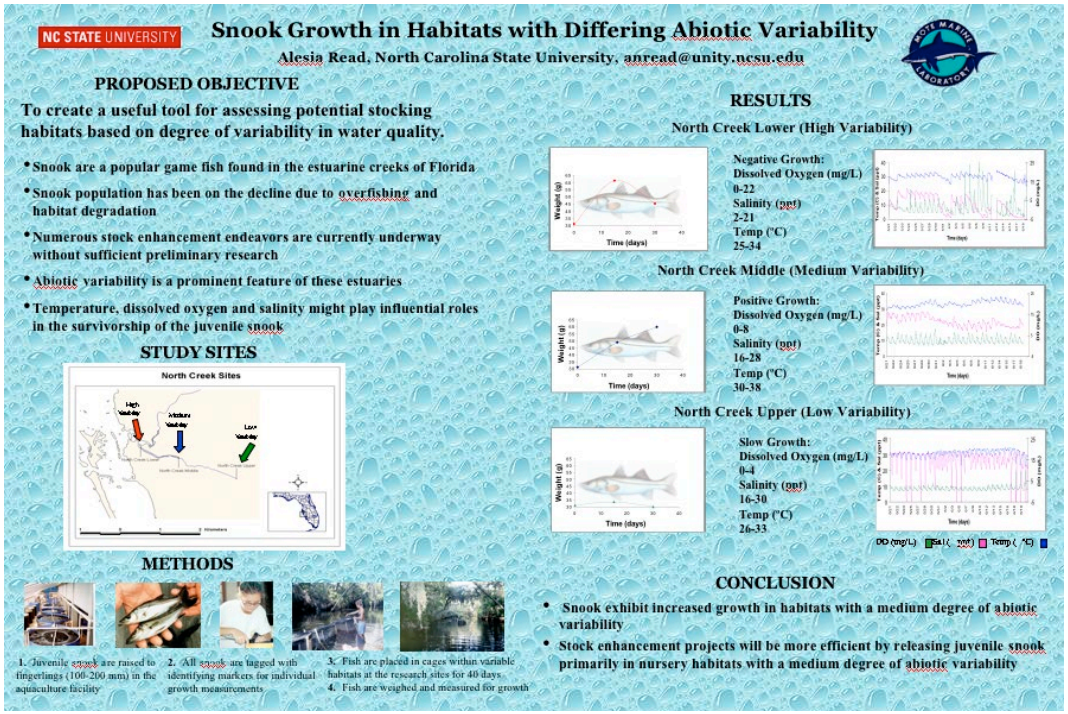

Last steps before printing

- Proof-reading!
- Print the poster on normal printer paper and go through it carefully – there is nothing worse than an obvious typo blown up to poster size

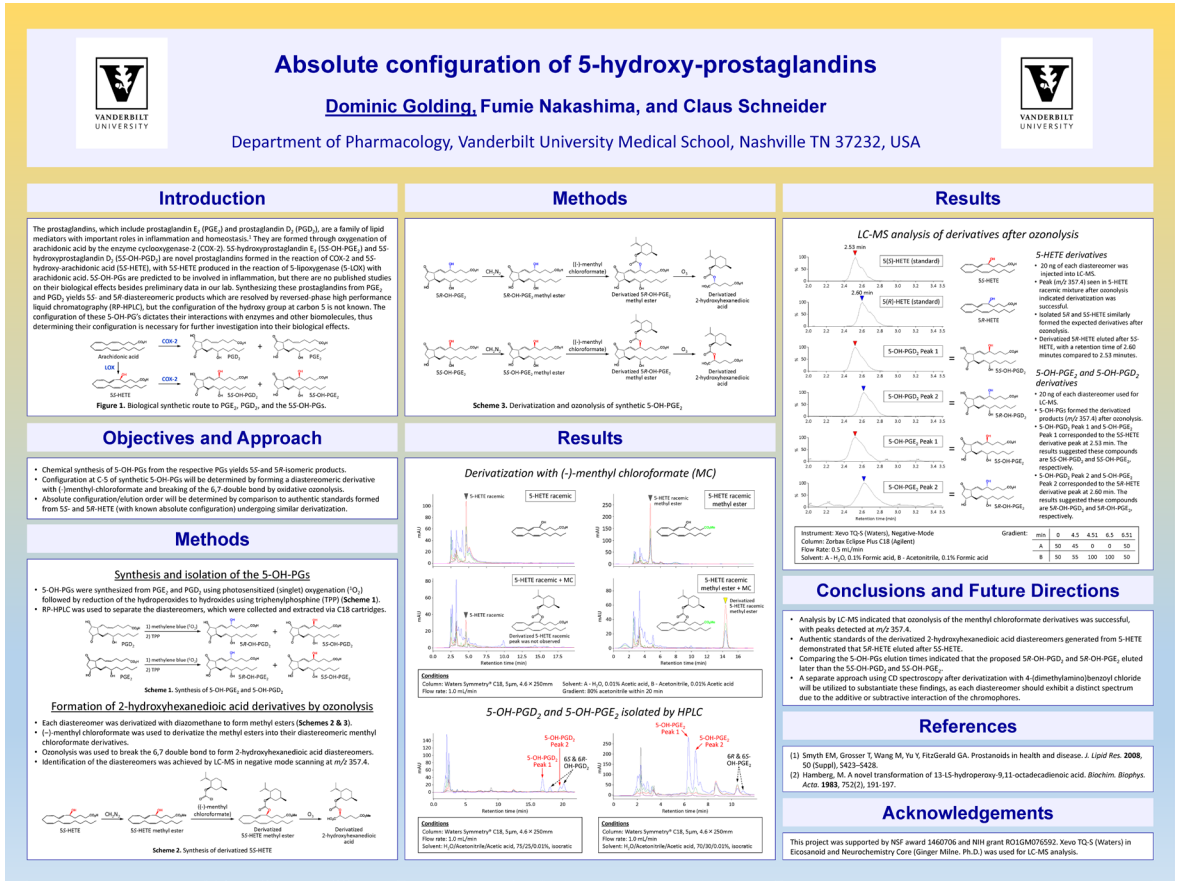

Absolute configuration of 5-hydroxy-prostaglandins

Dominic Golding, Fumie Nakashima, and Claus Schneider

Department of Pharmacology, Vanderbilt University Medical School, Nashville TN 37232, USA

Introduction

The prostaglandins, which include prostaglandin E_2 (PGE_2) and prostaglandin D_2 (PGD_2), are a family of lipid mediators with important roles in inflammation and homeostasis.[1] They are formed through oxygenation of arachidonic acid by the enzyme cyclooxygenase-2 (COX-2). 5*S*-hydroxyprostaglandin E_2 (5*S*-OH-PGE_2) and 5*S*-hydroxyprostaglandin D_2 (5*S*-OH-PGD_2) are novel prostaglandins formed in the reaction of COX-2 and 5*S*-hydroxy-arachidonic acid (5*S*-HETE), with 5*S*-HETE produced in the reaction of 5-lipoxygenase (5-LOX) with arachidonic acid. 5*S*-OH-PGs are predicted to be involved in inflammation, but there are no published studies on their biological effects besides preliminary data in our lab. Synthesizing these prostaglandins from PGE_2 and PGD_2 yields 5*S*- and 5*R*-diastereomeric products which are resolved by reversed-phase high performance liquid chromatography (RP-HPLC), but the configuration of the hydroxy group at carbon 5 is not known. The configuration of these 5-OH-PG's dictates their interactions with enzymes and other biomolecules, thus determining their configuration is necessary for further investigation into their biological effects.

Figure 1. Biological synthetic route to PGE_2, PGD_2, and the 5*S*-OH-PGs.

Objectives and Approach

- Chemical synthesis of 5-OH-PGs from the respective PGs yields 5*S*-and 5*R*-isomeric products.
- Configuration at C-5 of synthetic 5-OH-PGs will be determined by forming a diastereomeric derivative with (-)menthyl-chloroformate and breaking of the 6,7-double bond by oxidative ozonolysis.
- Absolute configuration/elution order will be determined by comparison to authentic standards formed from 5*S*- and 5*R*-HETE (with known absolute configuration) undergoing similar derivatization.

Methods

Synthesis and isolation of the 5-OH-PGs

- 5-OH-PGs were synthesized from PGE_2 and PGD_2 using photosensitized (singlet) oxygenation ($^1O_2$) followed by reduction of the hydroperoxides to hydroxides using triphenylphosphine (TPP) (**Scheme 1**).
- RP-HPLC was used to separate the diastereomers, which were collected and extracted via C18 cartridges.

Scheme 1. Synthesis of 5-OH-PGE_2 and 5-OH-PGD_2

Formation of 2-hydroxyhexanedioic acid derivatives by ozonolysis

- Each diastereomer was derivatized with diazomethane to form methyl esters (**Schemes 2 & 3**).
- (–)-menthyl chloroformate was used to derivatize the methyl esters into their diastereomeric menthyl chloroformate derivatives.
- Ozonolysis was used to break the 6,7 double bond to form 2-hydroxyhexanedioic acid diastereomers.
- Identification of the diastereomers was achieved by LC-MS in negative mode scanning at m/z 357.4.

Scheme 2. Synthesis of derivatized 5*S*-HETE

Methods

Scheme 3. Derivatization and ozonolysis of synthetic 5-OH-PGE_2

Results

Derivatization with (-)-menthyl chloroformate (MC)

Conditions
Column: Waters Symmetry® C18, 5µm, 4.6 × 250mm
Flow rate: 1.0 mL/min
Solvent: A - H_2O, 0.01% Acetic acid, B - Acetonitrile, 0.01% Acetic acid
Gradient: 80% acetonitrile within 20 min

5-OH-PGD_2 and 5-OH-PGE_2 isolated by HPLC

Conditions
Column: Waters Symmetry® C18, 5µm, 4.6 × 250mm
Flow rate: 1.0 mL/min
Solvent: H_2O/Acetonitrile/Acetic acid, 75/25/0.01%, isocratic

Conditions
Column: Waters Symmetry® C18, 5µm, 4.6 × 250mm
Flow rate: 1.0 mL/min
Solvent: H_2O/Acetonitrile/Acetic acid, 70/30/0.01%, isocratic

Results

LC-MS analysis of derivatives after ozonolysis

5-HETE derivatives

- 20 ng of each diastereomer was injected into LC-MS.
- Peak (m/z 357.4) seen in 5-HETE racemic mixture after ozonolysis indicated derivatization was successful.
- Isolated 5*R* and 5*S*-HETE similarly formed the expected derivatives after ozonolysis.
- Derivatized 5*R*-HETE eluted after 5*S*-HETE, with a retention time of 2.60 minutes compared to 2.53 minutes.

5-OH-PGE_2 and 5-OH-PGD_2 derivatives

- 20 ng of each diastereomer used for LC-MS.
- 5-OH-PGs formed the derivatized products (m/z 357.4) after ozonolysis.
- 5-OH-PGD_2 Peak 1 and 5-OH-PGE_2 Peak 1 corresponded to the 5*S*-HETE derivative peak at 2.53 min. The results suggested these compounds are 5*S*-OH-PGD_2 and 5*S*-OH-PGE_2, respectively.
- 5-OH-PGD_2 Peak 2 and 5-OH-PGE_2 Peak 2 corresponded to the 5*R*-HETE derivative peak at 2.60 min. The results suggested these compounds are 5*R*-OH-PGD_2 and 5*R*-OH-PGE_2, respectively.

Instrument: Xevo TQ-S (Waters), Negative-Mode
Column: Zorbax Eclipse Plus C18 (Agilent)
Flow Rate: 0.5 mL/min
Solvent: A - H_2O, 0.1% Formic acid, B - Acetonitrile, 0.1% Formic acid

Gradient:

min	0	4.5	4.51	6.5	6.51
A	50	45	0	0	50
B	50	55	100	100	50

Conclusions and Future Directions

- Analysis by LC-MS indicated that ozonolysis of the menthyl chloroformate derivatives was successful, with peaks detected at m/z 357.4.
- Authentic standards of the derivatized 2-hydroxyhexanedioic acid diastereomers generated from 5-HETE demonstrated that 5*R*-HETE eluted after 5*S*-HETE.
- Comparing the 5-OH-PGs elution times indicated that the proposed 5*R*-OH-PGD_2 and 5*R*-OH-PGE_2 eluted later than the 5*S*-OH-PGD, and 5*S*-OH-PGE_2.
- A separate approach using CD spectroscopy after derivatization with 4-(dimethylamino)benzoyl chloride will be utilized to substantiate these findings, as each diastereomer should exhibit a distinct spectrum due to the additive or subtractive interaction of the chromophores.

References

(1) Smyth EM, Grosser T, Wang M, Yu Y, FitzGerald GA. Prostanoids in health and disease. *J. Lipid Res.* **2008**, 50 (Suppl), S423–S428.

(2) Hamberg, M. A novel transformation of 13-LS-hydroperoxy-9,11-octadecadienoic acid. *Biochim. Biophys. Acta.* **1983**, 752(2), 191-197.

Acknowledgements

This project was supported by NSF award 1460706 and NIH grant R01GM076592. Xevo TQ-S (Waters) in Eicosanoid and Neurochemistry Core (Ginger Milne. Ph.D.) was used for LC-MS analysis.

VANDERBILT UNIVERSITY

Last step = Practice your 5 minute talk

- Over and Over again!
- Practice it out loud to yourself a few times and then to your friends!

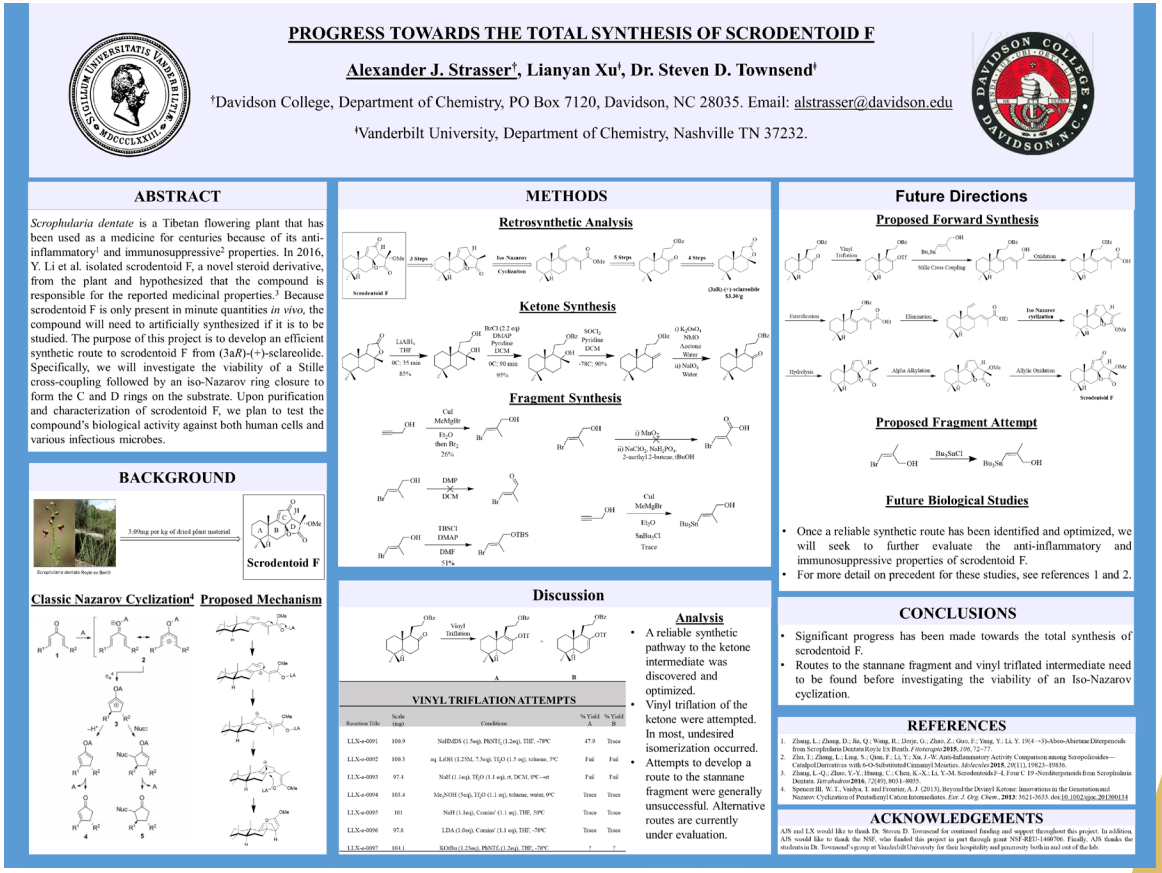

PROGRESS TOWARDS THE TOTAL SYNTHESIS OF SCRODENTOID F

Alexander J. Strasser†, Lianyan Xu‡, Dr. Steven D. Townsend‡

†Davidson College, Department of Chemistry, PO Box 7120, Davidson, NC 28035. Email: alstrasser@davidson.edu

‡Vanderbilt University, Department of Chemistry, Nashville TN 37232.

ABSTRACT

Scrophularia dentate is a Tibetan flowering plant that has been used as a medicine for centuries because of its anti-inflammatory[1] and immunosuppressive[2] properties. In 2016, Y. Li et al. isolated scrodentoid F, a novel steroid derivative, from the plant and hypothesized that the compound is responsible for the reported medicinal properties.[3] Because scrodentoid F is only present in minute quantities *in vivo*, the compound will need to artificially synthesized if it is to be studied. The purpose of this project is to develop an efficient synthetic route to scrodentoid F from (3a*R*)-(+)-sclareolide. Specifically, we will investigate the viability of a Stille cross-coupling followed by an iso-Nazarov ring closure to form the C and D rings on the substrate. Upon purification and characterization of scrodentoid F, we plan to test the compound's biological activity against both human cells and various infectious microbes.

BACKGROUND

3.99mg per kg of dried plant material

Scrodentoid F

Classic Nazarov Cyclization[4]

Proposed Mechanism

METHODS

Retrosynthetic Analysis

Ketone Synthesis

Fragment Synthesis

Discussion

VINYL TRIFLATION ATTEMPTS

Reaction Title	Scale (mg)	Conditions	% Yield A	% Yield B
LLX-e-0091	100.9	NaHMDS (1.5eq), PhNTf$_2$ (1.2eq), THF, -78ºC	47.9	Trace
LLX-e-0092	100.3	aq. LiOH (1.25M, 7.5eq), Tf$_2$O (1.5 eq), toluene, 5ºC	Fail	Fail
LLX-e-0093	97.4	NaH (1.1eq), Tf$_2$O (1.1 eq), rt, DCM, 0ºC→rt	Fail	Fail
LLX-e-0094	103.4	Me$_3$NOH (5eq), Tf$_2$O (1.1 eq), toluene, water, 0ºC	Trace	Trace
LLX-e-0095	101	NaH (1.1eq), Cousins' (1.1 eq), THF, 50ºC	Trace	Trace
LLX-e-0096	97.8	LDA (1.0eq), Cousins' (1.1 eq), THF, -78ºC	Trace	Trace
LLX-e-0097	101.1	KOtBu (1.25eq), PhNTf$_2$ (1.2eq), THF, -78ºC	?	?

Analysis

- A reliable synthetic pathway to the ketone intermediate was discovered and optimized.
- Vinyl triflation of the ketone were attempted. In most, undesired isomerization occurred.
- Attempts to develop a route to the stannane fragment were generally unsuccessful. Alternative routes are currently under evaluation.

Future Directions

Proposed Forward Synthesis

Proposed Fragment Attempt

Future Biological Studies

- Once a reliable synthetic route has been identified and optimized, we will seek to further evaluate the anti-inflammatory and immunosuppressive properties of scrodentoid F.
- For more detail on precedent for these studies, see references 1 and 2.

CONCLUSIONS

- Significant progress has been made towards the total synthesis of scrodentoid F.
- Routes to the stannane fragment and vinyl triflated intermediate need to be found before investigating the viability of an Iso-Nazarov cyclization.

REFERENCES

1. Zhang, L.; Zhang, D.; Jin, Q.; Wang, R.; Dorje, G.; Zhao, Z.; Guo, F.; Yang, Y.; Li, Y. 19(4→3)-Abeo-Abietane Diterpenoids from Scrophularia Dentata Royle Ex Benth. *J Nat Prod* **2015**, *78*, 72–77.
2. Zhu, T.; Zhang, L.; Ling, S.; Qian, F.; Li, Y.; Xu, J.-W. Anti-Inflammatory Activity Comparison among Scropolioside—Catalpol Derivatives with 6-O-Substituted Cinnamoyl Moieties. *Molecules* **2015**, *20* (11), 19823–19836.
3. Zhang, L.-Q.; Zhao, Y.-Y.; Huang, C.; Chen, K.-X.; Li, Y.-M. Scrodentoids F–I, Four C 19 -Norditerpenoids from Scrophularia Dentata. *Tetrahedron* **2016**, *72* (8), 8011–8015.
4. Spencer III, W. T., Vaidya, T. and Frontier, A. J. (2013), Beyond the Divinyl Ketone: Innovations in the Generation and Nazarov Cyclization of Pentadienyl Cation Intermediates. *Eur. J. Org. Chem.*, **2013**: 3621-3633. doi:10.1002/ejoc.201300134

ACKNOWLEDGEMENTS

AJS and LX would like to thank Dr. Steven D. Townsend for continued funding and support throughout this project. In addition, AJS would like to thank the NSF who funded this project in part through grant NSF-REU-1460706. Finally, AJS thanks the students in Dr. Townsend's group at Vanderbilt University for their hospitality and generosity both in and out of the lab.

VANDERBILT UNIVERSITY

Virtual Poster Sessions and Short Presentations

- If you are not giving an in-person poster, most of this still applies accept formatting the story on a poster board
- You'll need to think of what graphics to include, what story you want to tell and you'll want to practice your 5-minute talk, walking through your research step by step

VANDERBILT UNIVERSITY

Day of the Poster Session

- Be excited to show off your work!
- Actively engage during the session, remember to ask if they'd like to hear about your poster to start
- Feel free to ask "have I been clear enough?" "should I go into more detail?" to make the presentation more interactive

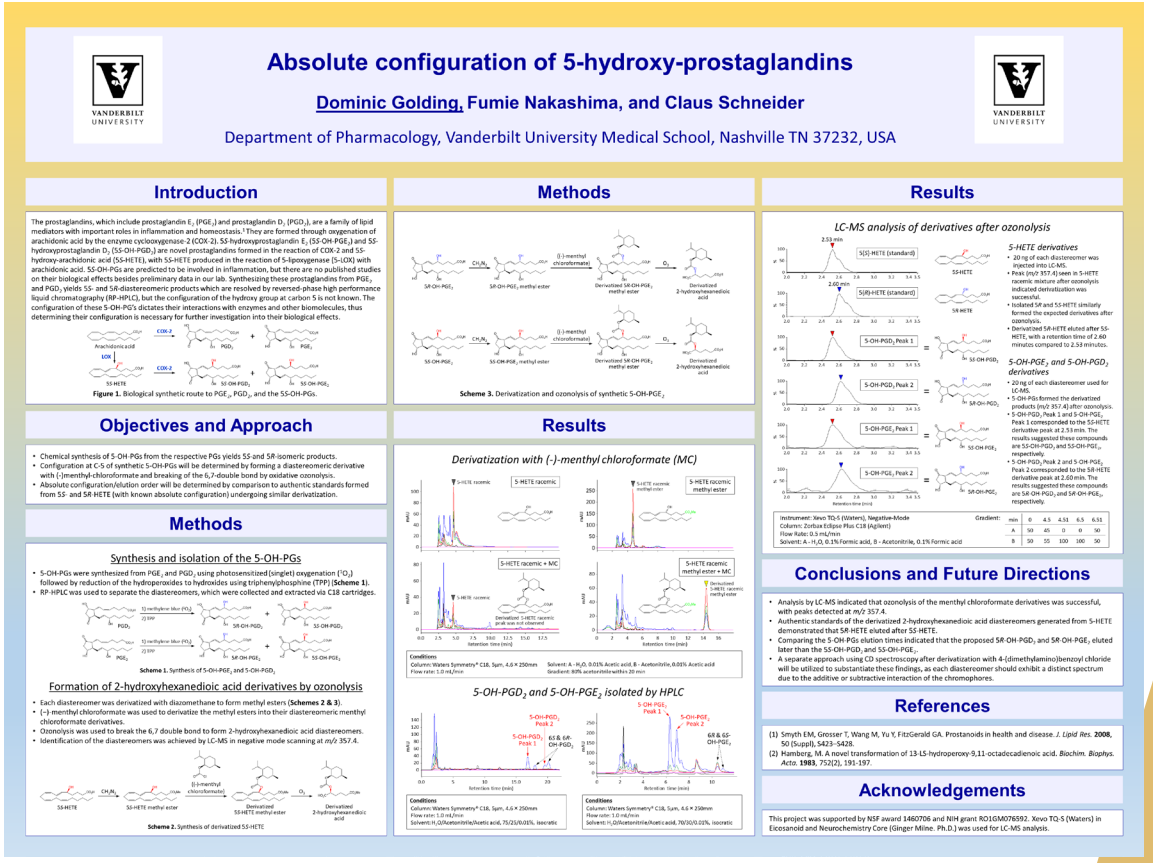

Absolute configuration of 5-hydroxy-prostaglandins

Dominic Golding, Fumie Nakashima, and Claus Schneider

Department of Pharmacology, Vanderbilt University Medical School, Nashville TN 37232, USA

Introduction

The prostaglandins, which include prostaglandin E_2 (PGE_2) and prostaglandin D_2 (PGD_2), are a family of lipid mediators with important roles in inflammation and homeostasis.[1] They are formed through oxygenation of arachidonic acid by the enzyme cyclooxygenase-2 (COX-2). 5*S*-hydroxyprostaglandin E_2 (5*S*-OH-PGE_2) and 5*S*-hydroxyprostaglandin D_2 (5*S*-OH-PGD_2) are novel prostaglandins formed in the reaction of COX-2 and 5*S*-hydroxy-arachidonic acid (5*S*-HETE), with 5*S*-HETE produced in the reaction of 5-lipoxygenase (5-LOX) with arachidonic acid. 5*S*-OH-PGs are predicted to be involved in inflammation, but there are no published studies on their biological effects besides preliminary data in our lab. Synthesizing these prostaglandins from PGE_2 and PGD_2 yields 5*S*- and 5*R*-diastereomeric products which are resolved by reversed-phase high performance liquid chromatography (RP-HPLC), but the configuration of the hydroxy group at carbon 5 is not known. The configuration of these 5-OH-PG's dictates their interactions with enzymes and other biomolecules, thus determining their configuration is necessary for further investigation into their biological effects.

Arachidonic acid → (COX-2) → PGD_2 + PGE_2

Arachidonic acid → (LOX) → 5*S*-HETE → (COX-2) → 5*S*-OH-PGD_2 + 5*S*-OH-PGE_2

Figure 1. Biological synthetic route to PGE_2, PGD_2, and the 5*S*-OH-PGs.

Objectives and Approach

- Chemical synthesis of 5-OH-PGs from the respective PGs yields 5*S*- and 5*R*-isomeric products.
- Configuration at C-5 of synthetic 5-OH-PGs will be determined by forming a diastereomeric derivative with (-)-menthyl-chloroformate and breaking of the 6,7-double bond by oxidative ozonolysis.
- Absolute configuration/elution order will be determined by comparison to authentic standards formed from 5*S*- and 5*R*-HETE (with known absolute configuration) undergoing similar derivatization.

Methods

Synthesis and isolation of the 5-OH-PGs

- 5-OH-PGs were synthesized from PGE_2 and PGD_2 using photosensitized (singlet) oxygenation ($^1O_2$) followed by reduction of the hydroperoxides to hydroxides using triphenylphosphine (TPP) (**Scheme 1**).
- RP-HPLC was used to separate the diastereomers, which were collected and extracted via C18 cartridges.

PGD_2 → (1) methylene blue (5%), (2) hν → 5*R*-OH-PGD_2 + 5*S*-OH-PGD_2

PGE_2 → (1) methylene blue (5%), (2) hν → 5*R*-OH-PGE_2 + 5*S*-OH-PGE_2

Scheme 1. Synthesis of 5-OH-PGE_2 and 5-OH-PGD_2

Formation of 2-hydroxyhexanedioic acid derivatives by ozonolysis

- Each diastereomer was derivatized with diazomethane to form methyl esters (**Schemes 2 & 3**).
- (-)-menthyl chloroformate was used to derivatize the methyl esters into their diastereomeric menthyl chloroformate derivatives.
- Ozonolysis was used to break the 6,7 double bond to form 2-hydroxyhexanedioic acid diastereomers.
- Identification of the diastereomers was achieved by LC-MS in negative mode scanning at *m/z* 357.4.

5*S*-HETE → (CH_2N_2) → 5*S*-HETE methyl ester → ((-)-menthyl chloroformate) → Derivatized 5*S*-HETE methyl ester → (O_3) → Derivatized 2-hydroxyhexanedioic acid

Scheme 2. Synthesis of derivatized 5*S*-HETE

Methods

5-OH-PGE_2 → (CH_2N_2) → 5-OH-PGE_2 methyl ester → ((-)-menthyl chloroformate) → Derivatized 5-OH-PGE_2 methyl ester → (O_3) → Derivatized 2-hydroxyhexanedioic acid

5-OH-PGD_2 → (CH_2N_2) → 5-OH-PGD_2 methyl ester → ((-)-menthyl chloroformate) → Derivatized 5-OH-PGD_2 methyl ester → (O_3) → Derivatized 2-hydroxyhexanedioic acid

Scheme 3. Derivatization and ozonolysis of synthetic 5-OH-PGE_2

Results

Derivatization with (-)-menthyl chloroformate (MC)

Conditions
Column: Waters Symmetry® C18, 5µm, 4.6 × 250mm
Flow rate: 1.0 mL/min
Solvent: A - H_2O, 0.01% Acetic acid, B - Acetonitrile, 0.01% Acetic acid
Gradient: 80% acetonitrile within 20 min

5-OH-PGD_2 and 5-OH-PGE_2 isolated by HPLC

Conditions
Column: Waters Symmetry® C18, 5µm, 4.6 × 250mm
Flow rate: 1.0 mL/min
Solvent: H_2O/Acetonitrile/Acetic acid, 75/25/0.01%, isocratic

Conditions
Column: Waters Symmetry® C18, 5µm, 4.6 × 250mm
Flow rate: 1.0 mL/min
Solvent: H_2O/Acetonitrile/Acetic acid, 70/30/0.01%, isocratic

Results

LC-MS analysis of derivatives after ozonolysis

5-HETE derivatives

- 20 ng of each diastereomer was injected into LC-MS.
- Peak (*m/z* 357.4) seen in 5-HETE racemic mixture after ozonolysis indicated derivatization was successful.
- Isolated 5*R* and 5*S*-HETE similarly formed the expected derivatives after ozonolysis.
- Derivatized 5*R*-HETE eluted after 5*S*-HETE, with a retention time of 2.60 minutes compared to 2.53 minutes.

5-OH-PGE_2 and 5-OH-PGD_2 derivatives

- 20 ng of each diastereomer used for LC-MS.
- 5-OH-PGs formed the derivatized products (*m/z* 357.4) after ozonolysis.
- 5-OH-PGD_2 Peak 1 and 5-OH-PGE_2 Peak 1 corresponded to the 5*S*-HETE derivative peak at 2.53 min. The results suggested these compounds are 5*S*-OH-PGD_2 and 5*S*-OH-PGE_2, respectively.
- 5-OH-PGD_2 Peak 2 and 5-OH-PGE_2 Peak 2 corresponded to the 5*R*-HETE derivative peak at 2.60 min. The results suggested these compounds are 5*R*-OH-PGD_2 and 5*R*-OH-PGE_2, respectively.

Instrument: Xevo TQ-S (Waters), Negative-Mode
Column: Zorbax Eclipse Plus C18 (Ag/em)
Flow Rate: 0.5 mL/min
Solvent: A - H_2O, 0.1% Formic acid, B - Acetonitrile, 0.1% Formic acid

Gradient:

min	0	4.5	4.51	6.5	6.51
A	50	45	0	0	50
B	50	55	100	100	50

Conclusions and Future Directions

- Analysis by LC-MS indicated that ozonolysis of the menthyl chloroformate derivatives was successful, with peaks detected at *m/z* 357.4.
- Authentic standards of the derivatized 2-hydroxyhexanedioic acid diastereomers generated from 5-HETE demonstrated that 5*R*-HETE eluted after 5*S*-HETE.
- Comparing the 5-OH-PGs elution times indicated that the proposed 5*R*-OH-PGD_2 and 5*R*-OH-PGE_2 eluted later than the 5*S*-OH-PGD, and 5*S*-OH-PGE_2.
- A separate approach using CD spectroscopy after derivatization with 4-(dimethylamino)benzoyl chloride will be utilized to substantiate these findings, as each diastereomer should exhibit a distinct spectrum due to the additive or subtractive interaction of the chromophores.

References

(1) Smyth EM, Grosser T, Wang M, Yu Y, FitzGerald GA. Prostanoids in health and disease. *J. Lipid Res.* **2008**, 50 (Suppl), S423–S428.
(2) Hamberg, M. A novel transformation of 13-LS-hydroperoxy-9,11-octadecadienoic acid. *Biochim. Biophys. Acta.* **1983**, 752(2), 191-197.

Acknowledgements

This project was supported by NSF award 1460706 and NIH grant RO1GM076592. Xevo TQ-S (Waters) in Eicosanoid and Neurochemistry Core (Ginger Milne. Ph.D.) was used for LC-MS analysis.

VANDERBILT UNIVERSITY

Day of the Poster Session

Dealing with feedback

- It is important to welcome feedback, be prepared for discussion and not to be too defensive in the face of criticism.

- If someone asks you a question or makes a comment that you don't think is relevant, ask them to explain the relevance of their comment. They may have stumbled across something that you haven't thought of because of their fresh perspective on the topic, or they might just not understand your research.

- Remember to thank the audience for listening and thank them for their feedback. **Assume that they are trying to help!**

Getting Started

1. Try to tell the story through graphics!
   - Which plots, graphs and other images will help you get the story across?
2. Make an outline first

Background
- Frame the research problem
- Why should the listener care
- Is there a graph or chart that can fit here?

Methods
- Explain how you are doing the research
- Define methods and don't assume your listener understands how the experiments are run

Results
- Focus on 3-4 main results
- Use graphics to support your claims = charts, graphs, pictures

Key Takeaways
- What have you concluded from the experiments above?
- What is next?

LET'S JUDGE SOME DESIGNS

Using a Windbreak Habitat Model Across Broad Landscapes: The Effect of Local Landscape Composition and Geographic Location

George Hess[1], John Poulsen[2], Raymond O'Connor[2], Jeff Bay[3]

1. Windbreaks as Habitat

Agricultural lands -- fields, pastures, and orchards -- are managed to produce food and fiber for people. In the U.S. Great Plains, an extensive agricultural landscape, windbreaks have been planted to protect fields, crops, livestock, and farmsteads from the prevailing winds. ***Windbreaks provide some of the scarce wooded habitat for birds and other wildlife that people have come to value.*** Windbreaks make up about 25% of the wooded cover in Nebraska; much of the other wooded cover occurs along riparian corridors.

Although they protect soil from wind erosion and provide habitat for some species, windbreaks also contribute to the fragmentation of prairie grasslands. Prairie fragmentation negatively impacts grassland wildlife such as greater prairie chickens, upland sandpipers, and prongborn antelope.

2. Regional Evaluation of Windbreaks

The Environmental Monitoring and Assessment Program's Agricultural Lands Group -- charged with assessing the ecological condition of U.S. agricultural lands -- undertook a ***pilot study to evaluate the habitat value of windbreaks on a regional basis.*** We decided to use a bird species richness index to measure the habitat value of individual windbreaks.

We selected a random sample of 60 windbreaks in Nebraska, based on a screening question on a USDA National Agricultural Statistics Service agricultural survey. In July 1994, field crews measured attributes of 40 windbreaks (one third of the farmers refused to participate). The data were used to estimate the value of windbreaks as breeding bird habitat in Nebraska.

3. Bird Species Richness Index

We used the U.S. Fish and Wildlife Service's Bird Species Richness Index (BSRI), which ***estimates the number of breeding bird species a single windbreak can support based on four windbreak attributes.***

- ***Area*** has the greatest impact on bird diversity; larger windbreaks support more species. Area was ***measured by calibrated pacing.***
- ***Height:*** Taller windbreaks provide more niches. Height was ***measured by photographic analysis.***
- ***Vertical Structure:*** A more structurally complex windbreak provides more habitat niches; ***measured by point sampling.***
- ***Snags*** provide another habitat niche. ***Snags*** were censused.

- **Forty windbreaks were sampled using two-stage sampling with a frame stratified by intensity of cultivation.**
- **Most sample windbreaks fell in or near extensive cropland.**
- **Habitat characteristics of each windbreak were measured in 1994.**
- **Thirty-five farmers allowed ornithologists to return in 1995**

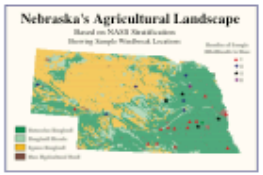

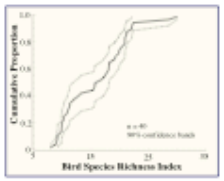

- **Using expansion factors associated with each sample, we estimated the habitat value of windbreaks for the region (graph left).**
- **We estimated that half of Nebraska's windbreaks support fewer than 10 breeding bird species (graph left).**
- **We also estimated that between 87% and 100% of windbreaks are smaller than 1.5 hectares (data not shown), suggesting that few Nebraskan windbreaks provide habitat for forest interior or area sensitive birds.**

4. Validating BSRI Model

In 1995, a team of five ***ornithologists revisited 35 of the 40 windbreaks*** (5 farmers refused further visits) between late May and early July.

Each windbreak was visited four times. Data were collected between one-half hour before and four hours after sunrise. ***All observed birds were identified to species and recorded using spot mapping techniques.*** Tape recorded vocalizations of the eastern screech owl were played on the final pass through the windbreak for each visit.

Because the windbreaks were narrow, we assumed all species were detected.

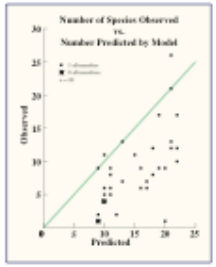

5. Results of Validation

The model overestimates the number of bird species in the Nebraska windbreaks (graph left). However, the relative qualitative ranking of windbreaks is generally preserved. A total of 91 species were observed.

No strong, significant relationship was found between deviation of observed from predicted number of species and any windbreak attribute or the geographic location of individual windbreaks.

Forest-interior, area-sensitive, and forest-edge species occurred in the larger, taller, more complex windbreaks.

Open-land and grassland species occurred in the smaller, shorter, less complex windbreaks.

6. Failure of the Model

There are several ***possible explanations*** for the failure of the model to predict accurately the number of birds species in the windbreaks.

1) ***Geographic differences in species richness.*** The model was developed in Kansas, which has 5-20 more species of bird than Nebraska (Breeding Bird Survey's species richness map of North America).

2) ***Dependence on different windbreak characteristics.*** The number of species in Nebraska's windbreaks depends *differently* on windbreak characteristics than did the number of species in Kansas.

3) ***Dependence on landscape-scale characteristics.*** The number of species in Nebraska's windbreaks depends on characteristics of the surrounding landscape.

7. Local Landscape-Scale Effects

Land cover data were collected for the quarter-section (160 acres, 65 ha) containing the sample windbreak. Cover categories were tree, wetland, crop, grass / herbaceous, barren (non-vegetated), and water. Fences and cattle grazing were also recorded (present / absent).

Landscape metrics computed included relative cover distributions, total edge length, edge / area ratios, number of patches, mean patch size, mean perimeter per patch, and size of largest field.

The deviation between observed and predicted number of species was not significantly related to any of the landscape metrics. This suggests that within a region the number of species using a windbreak depends primarily on windbreak attributes.

8. Conclusions

1) ***The Bird Species Richness Index for windbreaks cannot be extended simply to describe species richness at large regional scales*** without either recalibrating regionally or adding terms that account for differences in regional species pools.

2) ***Local landscape-scale composition and structure do not explain the failure of the model.***

3) ***The presence of species guilds in windbreaks*** (e.g., forest interior, grassland) ***may be explained by windbreak size and complexity.*** The model may be more useful for predicting the presence or absence of species guilds than for predicting the total number of species present.

Acknowledgements: This work could not have been done without the many dedicated people at the National Agricultural Statistics Service who helped plan and execute the 1994 data collection effort; the kind farmers who allowed us to survey their windbreaks; the five ornithologists who spent six weeks traveling around Nebraska; and many other people from the University of Nebraska, U.S. Fish and Wildlife Service, Natural Resources Conservation Service, and the Environmental Protection Agency. Funding was provided by the Environmental Protection Agency and the USDA Agricultural Research Service.

1. North Carolina State University, Forestry Department, Raleigh, NC
2. University of Maine, Department of Wildlife Ecology, Orono, ME
3. North Carolina State University, Statistics Department, Raleigh, NC

17 March 1997

Determining the Wear Resistance of Occlusal Splints in a Prospective Clinical Study

P. Ottl, P. Schmelz, A. Piwowarczyk, H.-Ch. Lauer

Dept. of Prosthodontics, School of Dentistry (Director: Prof. Dr. H.-Ch. Lauer), ZZMK (Carolinum), J. W. Goethe University, Frankfurt, Germany

Objective

- To determine quantitatively the wear resistance of a newly developed light-curing splint resin over a period in situ of six months.

Materials and Methods

- **Patients**

  n = 20 consecutive patients

  (mean age: 34.7 years; 12 F, 8 M)

- **Inclusion criteria**

  - Natural dentition/fixed denture
  - Complete dentition to at least the 1st molar

  and

  for the stabilization splint sample:
  - Insufficient occlusal support
  - Increased occlusal loss of dental hard tissue

  for the distraction splint sample:
  - TMJ pain **and**
  - Complete anterior dislocation of the disk without reduction/with terminal reduction
  - TMJ osteoarthrosis

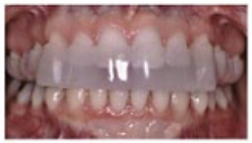

Fig. 1: Stabilization splint in situ

- **Resin splint material (Fig. 1)**
  - Light-curing (400–500 nm) resin made of high-molecular dimethacrylates with organic and inorganic fillers
  - Does not contain methyl methacrylate

- **Study design**
  - **Duration**: 6 months
  - **Types of splints** (maxilla, n = 10 each): stabilization splints, distraction splints
  - **Splint wear mode**: 24 hours
  - **Examinations**: before insertion (BI), at 4 weeks (4W), at 3 months (3M), at 6 months (6M)
  - **Occlusal adjustments** were restricted to the time before 4W.

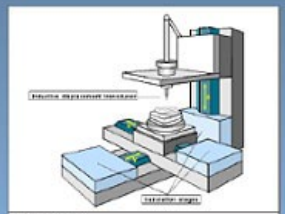

Fig. 2: Test setup

- **Measuring technology (Fig. 2)**
  - Vibration-isolated table framework
  - 3 translation stages (for directions x, y, and z) (DC-Motor) (Pl. Waldbronn)
  - DV 4 stereomicroscope (Zeiss, Oberkochen)
  - WA 20 inductive displacement transducer/ Spider8 digital 8-channel measurement unit/ Catman 32 software V2.1 (HBM, Darmstadt)
  - Local coordinate storage for occlusal contacts during baseline measurements
  - Ten measurements each in regions 13, 23, 16, 26 (BI, 4W, 3M, 6M)
  - Splint repositioned on remount cast

Results

- The medians of the occlusal vertical gains/losses (wear, resin torsion, water sorption, etc.) are shown in **Fig. 3** (stabilization splints) and **Fig. 4** (distraction splints).

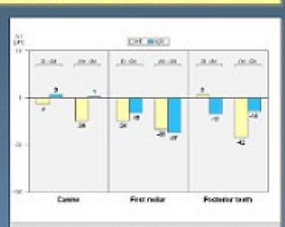

Fig. 3: Occlusal vertical gains/losses (medians) of the resin in vivo over a period in situ of six months (n = 10 stabilization splints)

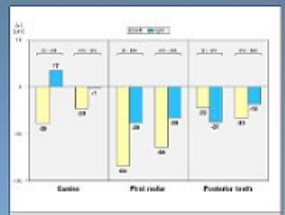

Fig. 4: Occlusal vertical gains/losses (medians) of the resin in vivo over a period in situ of six months (n = 10 distraction splints)

- **Statistical analysis** (Mann-Whitney U-test, $p \leq 0.05$) showed no significant differences when comparing the corresponding results of stabilization and distraction splints.

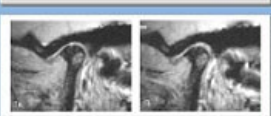

Figs. 5a and b: Sagittal oblique images (MRI) of the condyle/fossa relationship without splint (Fig. 5a) and with distraction splint inserted (Fig. 5b) following six months of wearing

Conclusions

- The present study *clinically* confirms the good wear resistance results of the new resin splint material obtained in a previous *in-vitro* study [OTTL et al., Dtsch Zahnärztl Z 52, 342 (1997)].
- Good wear resistance is of great importance for maintaining the therapeutic mandibular position during the treatment period (Figs. 5a and b).

A Framework for Assessing the Condition of Agricultural Lands

George Hess[1], Anne Hellkamp[2], Mike Munster[3], Steve Peck[3], Lee Campbell[3], Betty McQuaid[4], Steve Shafer[3,5]

Mission: To develop indicators of the condition of agricultural lands within an ecological framework, and to monitor and evaluate this condition on a regional basis.

Sustainable agriculture has been discussed, defined, and dissected in countless papers.

Definitions tend to be broad and encompass ecological, economic, social, and even policy dimensions. Although these dimensions are intertwined, each may be examined independently.

In our efforts, we sought methods to examine only the ecological aspects of sustainability.

People place values on agricultural lands that must be addressed if monitoring is to be relevant.

The foremost goal for agricultural lands is to produce food and fiber for human use.

Other desired outcomes can be considered goals for the larger landscape and sometimes functions as constraints on production. These *include clean air and water, wildlife habitat, and aesthetically pleasing landscapes.*

The ecological condition of agricultural land is defined by its productivity and the degree to which valued biotic and abiotic resources are conserved and protected.

Agricultural land in good condition is productive and does not compromise valued resources. Sustainability is the ability to maintain good condition over time.

Indicators were selected to reflect crop productivity and land stewardship.

In making an assessment, condition is reported for each indicator. An overall condition may also be reported, but depends critically on the relative weighting of the goals for agricultural lands.

For sustainability, one can examine trends in crop productivity and stewardship practices.

Potential Indicators for Annually Harvested Herbaceous Cropland

As a starting point, we chose to concentrate our efforts on developing indicators for ***annually harvested herbaceous cropland — land planted with crops that are harvested every year*** whether the plants are annual or perennial. Common examples are corn, wheat, soybeans, alfalfa hay, and strawberries.

We also endeavored to supplement, rather than duplicate, existing efforts. Our conceptual framework is flexible enough to incorporate indicators based on data from other monitoring efforts. For example, an erosion indicator could be developed using the USDA Natural Resources Conservation Service's Natural Resource Inventory data.

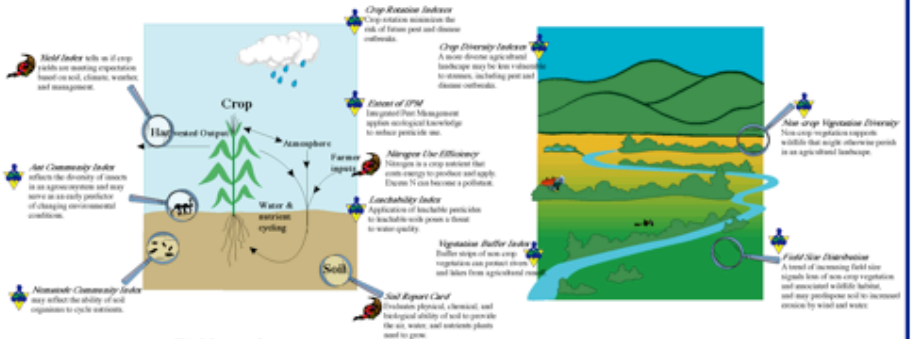

Fields are for crops . . .

. . . but landscapes are for all of us.

Acknowledgements: The EMAP Agricultural Lands Resource Group thanks the many individuals and organizations that made this effort a success. The individuals are too numerous to mention, but organizations include the USDA's Agricultural Research Service, Forest Service, National Agricultural Statistics Service, and Natural Resources Conservation Service; the U.S. Environmental Protection Agency; North Carolina State University, University of Maine, Oregon State University, University of Nebraska; and, well, I guess the list of organizations is pretty long, too. Thanks to all!!

1. North Carolina State University, Forestry Department, Raleigh NC
2. Duke University Medical Center, Durham NC
3. North Carolina State University, Department of Plant Pathology, Raleigh NC
4. USDA Natural Resources Conservation Service, Raleigh NC
5. USDA Agricultural Research Service, Raleigh NC

28 March 1997

PREVALENCE OF OBESITY AMONG INNER CITY LATINO CHILDREN AND ADOLESCENTS

Nazrat M. Mirza MD, ScD, Jill Merchant MS, Leila Beker, PhD

Children's National Medical Center and George Washington University School of Medicine and Health Sciences, Washington, DC

Background

Obesity is a major clinical and public health problem facing children and adolescents in the U.S. Of particular significance is the increasing prevalence of obesity and its complications among the Latino population. Among this ethnic group there is a strong sense of family, and children are a priority. Because of the premium placed on children, there may be a misplaced conception that children should not be denied food or other luxuries such as TV. Obesity in children and adolescents is concerning not only because of the associated health and psychosocial complications, but also because obese children tend to become obese adults. Since obesity is associated with many chronic diseases, it will have an enormous impact on the health care system.

Purpose of Study: To estimate the extent of obesity among inner city Latino children and adolescents with the overall goal of assessing the need for an obesity intervention program.

Study Design

One hundred and twenty five charts of children and adolescents aged 1 to 19 years were randomly selected from well child visits to Children's Hospital's Adams Morgan Clinic for the calendar year 2006. This clinic sees an average of 950-1000 patients a month, approximately 95-99% are Latinos, predominantly from El Salvador. Information extracted from the charts included weight, height, blood pressure, Tanner stage, dietary history and physical findings consistent with obesity complications. Body Mass Index (BMI) was calculated from recorded weight and height. Data analysis was done using SAS version 8.1.

Results

The distribution of the study sample is shown in Table 1. About 54% were females. The mean age was 11.6 years with a SD of 5.4 and a range of 1.8 to 18.7 years. The mean BMI was 20.8 with a SD of 5.8 and a range of 13.1 to 47.6. Overall 40% of the children and youth were overweight (BMI > 95th percentile) or at risk for overweight (BMI > 85-94th percentile), with an almost equal distribution between the two categories (Table 2). Males were more overweight and at risk for overweight than females, but the gender difference was not statistically significant. The prevalence of overweight was highest for youth ages 10 to 14 years.

Table 1 – Population statistics

Variable	Frequency %
Gender	
Males	46.4
Females	53.6
Age Category (years)	(n=125)
1–2	8.0
3–5	22.4
6–9	27.2
10–11	14.4
12–13	12.8
14–15	12.8
16–18	8.8

Table 2 – BMI distribution

BMI Category	Frequency %
At Risk for overweight: BMI= 85-94th%	
1. Both Sexes (n=125)	20.8
2. Males (n=58)	22.4
3. Females (n=67)	19.4
Overweight: BMI >95th Percentile	
1. Both Sexes (n=125)	19.2
2. Males (n=58)	24.1
3. Females (n=67)	14.9

Table 3 – At Risk for Overweight and Overweight by Age Category

Age Category (N=)	At Risk for Overweight (%) BMI 85-94th %	Overweight (%) BMI >95th %
1–2 y (n=10)	10.0	10.0
3–5 y (n=28)	28.6	21.4
6–10 y (n=52)	9.6	18.2
10–12y (n=18)	16.7	27.8
12–14y (n=17)	23.5	29.4
14–16y (n=11)	27.3	36.3
16–18 (n=9)	22.2	0.0

Results continued

Table 3 shows the distribution of overweight and at risk for overweight by age category. These data show that prevalence overweight and at risk for overweight is high in children as young as 9 to 9 years. Although the prevalence of overweight and at risk for overweight was lowest in the age group 3-5 years, the differences were not statistically significant (Fishers Exact test p=0.84 and p=0.08 respectively).

Asthma frequency was higher among the overweight than the non-overweight children and youth (p=0.08, Fishers Exact Test). There was no difference in the frequency of occurrence of other symptoms such as obstructive sleep apnea, learning difficulties, behavioral problems , anorexia, and ADHD between the overweight and non-overweight group. Only 7% of all the overweight children had their cholesterol levels checked. The cholesterol levels ranged from 112-199 mg/dl. Two percent of the children had their serum triglycerides assayed, and the range was 175-177 mg/dl. There was no significant association between overweight and systolic or diastolic blood pressure in this small sample. Only 20% of the overweight children and youth were diagnosed and notification made in their charts regarding their overweight status by their health care providers. There were no referrals for overweight intervention noted in their charts.

Conclusions & Recommendations

The prevalence rate for overweight and at risk for overweight among children and youth in this inner city Latino community is more than twice the national average. Primary health care providers need to acknowledge and accept the presence of obesity and overweight in children and adolescents early and provide appropriate management of the problem. Targeted intervention and prevention strategies for overweight and obesity in children and adolescents are urgently needed for this population.

Early Outcomes of the First 1471 Consecutive Kyphoplasty Procedures in the United States for the Fixation of Painful Osteopenic Vertebral Body Compression Fractures (VCF)

Steven R. Garfin[1], M.D., Isador H. Lieberman[2], M.D., Mark A. Reiley[3], M.D., Joseph M. Lane[4], M.D., Frank M. Phillips[5], M.D., Hallett B. Mathews[6], M.D., Hansen A. Yuan[7], M.D., Barton H. Sachs[8], M.D., for the Kyphoplasty Study Group

[1]University of California, San Diego, Medical Center, San Diego, CA, [2]Cleveland Clinic, Cleveland, OH, [3]Berkeley Orthopedic Medical Group, Berkeley, CA, [4]Hospital for Special Surgery, New York, NY, [5]University of Chicago Spine Center, Chicago, IL, [6]Mid-Atlantic Spine Specialists, Richmond, VA, [7]State University of New York Health Sciences Center, Syracuse, NY, [8]Albany Medical Center, Albany, NY

BACKGROUND

- 700,000 VCF's per year
- 275,000 diagnosed, >90% due to pain
- Spinal deformity associated with
  - Significant morbidity
  - 23% increased mortality (Kado, Ann Int Med 1999)
- Current treatments ineffective
  - Open surgeries fail
  - Medical management palliative
- Vertebroplasty
  - Bilateral transpedicular cement fill
  - Relieves pain
  - Requires high pressure and runny cement
  - High risk of cement leaks
    - Up to 73% where documented (Weill et al., Radiology 1997)
  - Major complications (Chiras, J Int Neurorad 1997)
    - 1.3% in osteoporosis
    - 10% in metastatic cancers

KYPHOPLASTY

Kyphoplasty is a minimally invasive orthopedic procedure for reducing and fixing painful vertebral body compression fractures secondary to osteopenia. Using a posterior approach, one or two Inflatable Bone Tamps (Fig. 1) are inserted into the fractured vertebral body, generally using a bilateral transpedicular approach (Fig. 2). The surgeon carefully inflates the balloon tamps (Fig. 2) using radiopaque contrast medium with image, volume and pressure control. The increased balloon tamp volume compacts the inner cancellous bone as it pushes the fractured outer cortical bone back toward its normal position. The inflation path is also controlled by placement, volume and balloon design. After reduction, the balloon tamp is removed, and the resulting void is filled with thick PMMA under fine manual control and low pressure. The steps of Kyphoplasty are illustrated in Fig 3.

KyphX™ Inflatable Bone Tamp (IBT)

Fig. 1

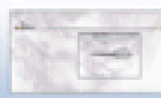

Cleared in the U.S. for the reduction of fractures and/or creation of a void in cancellous bone

Fig. 2

Bilateral Transpedicular Fracture Reduction with the IBT

Fig. 3 Kyphoplasty Using the IBT

STUDY DESIGN AND METHODS

A retrospective multi-center review to assess early outcomes with Kyphoplasty. Pain was localized by physical examination. The presence of marrow edema and collapse was confirmed on MRI. General or deep local anesthesia was chosen based on anatomy, number of levels and patient status. The first 135 patients at our centers were asked to characterize their back pain as improved, the same or worse 24 hours post-op and at last follow-up. Fractured and nearest normal vertebral body heights were measured anterior, midline and posterior in the first 27 vertebral body fractures treated by one surgeon (MAR). The height of the nearest normal vertebral body was used to calculate the % of predicted height for all the vertebral bodies (Fig. 4A) and for the sub-set where which had lost 15% or more of height before treatment (Fig. 4B).

The pre-treatment height was subtracted from the predicted height, then divided by the post-treatment height subtracted from the predicted height, to find the percentage of lost height restored. One set of X-rays by one surgeon (FMP) are used to show an example height restoration (Fig. 5A) and deformity correction (Fig. 5B). Device-related major complications from all procedures are reported. PMMA leaks in the first 70 procedures performed by one surgeon (IHL) were assessed with X-ray and MRI.

Figure 4A
Percent of Predicted Height Pre- and Post-Kyphoplasty (n=27)

Figure 4B
Percent of Predicted Height Pre- and Post-Kyphoplasty in Fractures With a 15% or Greater Compression

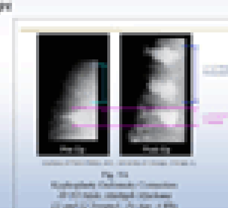

Fig. 5A
Kyphoplasty Deformity Correction

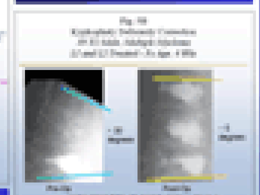

Fig. 5B
Kyphoplasty Deformity Correction

PRELIMINARY RESULTS

- 1471 fractures (Table 1)
  - Average fracture age: [illegible] months
  - Range: [illegible] days to [illegible] years
- [illegible] operations
- [illegible] patients (Table 2)
- Average no. levels/op: [illegible]
- Average injection pressure: [illegible] (range [illegible])
- Average Tamp inflation volume: [illegible] (range [illegible])
- More than 90% experience pain relief
  - Most immediately
- [illegible] report pain improvement at [illegible] months
- [illegible] restoration of lost height (Fig. 4A, 4B, 5A, 5B)
- No increased incidence of adjacent fracture
- [illegible] device related major complications
  - [illegible] neurological
  - [illegible] pulmonary
  - [illegible] bleeding
  - [illegible] deaths
- [illegible] leak rate [illegible]

CONCLUSIONS

Kyphoplasty is an important treatment option that provides immediate mobility and return to activities of daily living to patients with acutely painful vertebral body compression fractures secondary to osteopenia. Kyphoplasty facilitates fracture reduction and deformity correction. While reduction is more likely in acute fractures (four months or less), it has been seen in fractures over one year old. Kyphoplasty also provides rapid pain relief in the nearly all patients, and this result is independent of fracture reduction. The safety profile of Kyphoplasty compares favorably to the published safety profile of vertebroplasty.

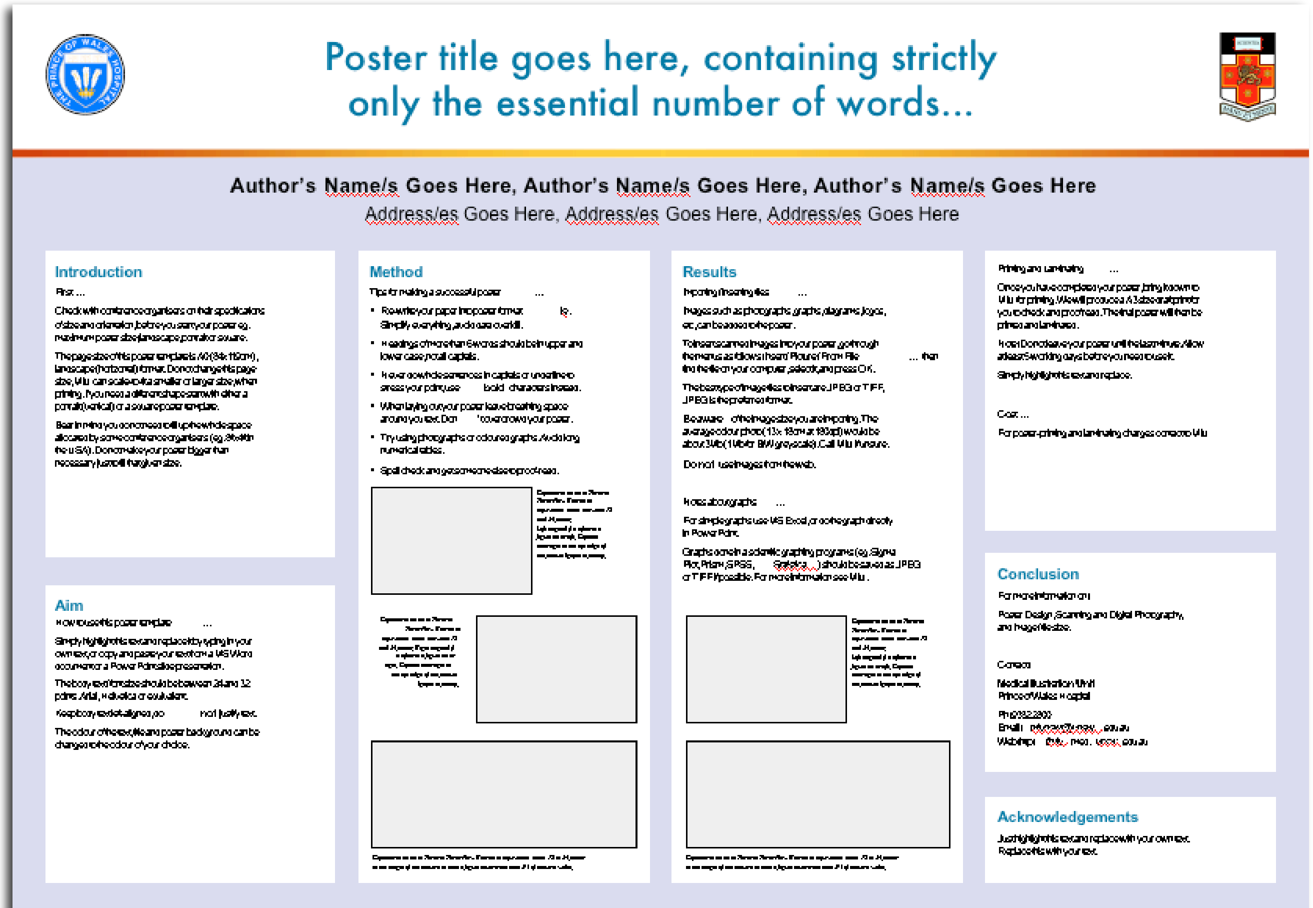
Poster title goes here, containing strictly only the essential number of words...
Author's Name/s Goes Here, Author's Name/s Goes Here, Author's Name/s Goes Here
Address/es Goes Here, Address/es Goes Here, Address/es Goes Here
Introduction
Method
Results
Aim
Conclusion
Acknowledgements


A Large-Scale Public Library Renovation in Taiwan
A Large Scale Public Library Renovation in Taiwan
Library Association of R.O.C.
National Taichung Library of Taiwan
ABSTRACT
In order to upgrade the quality of public library services in Taiwan to meet users needs and to fulfill lifelong learning, in 2002, the central government of Taiwan approved a budget of NT$1.2 billion (US$ 4 million) as a large-scale public library renovation project in 301 public libraries.
National Taichung Library was designated as coordinate library to execute the project from February 2003 to June 2004. 301 public libraries were divided into eight groups according to the geographical area, and a steering committee was formed, consisting 96 committee members from the fields of library and information science, architecture, space design, literature, and history. 96 committee members were assigned to one of eight groups of 301 public libraries to help and to give suggestions of renovation, improvement, replacement, service programs of each library.
The project was executed and completed efficiently and effectively in June 2004. This poster presentation will display the results of the renovation, improvement, replacement, library management, and services of 301 public libraries in Taiwan. The contents of the posters will be explained by words, pictures, and statistical tables.
Keyword: Public libraries
http://www.ntl.gov.tw
Background
Figure 1 : Number of Public libraries in Taiwan
How to achieve the project
Objectives
Distinguishing features of plan implementation
Implementation period : February 2003 thru June 2004
Performance
Future outlook
www.ntl.gov.tw

WHICH IS MORE IMPORTANT: NUMBER OF PATCHES OR CONNECTIVITY?

Darin Kalisak, PBS Student

INTRODUCTION AND OBJECTIVES

THE PROGRAM

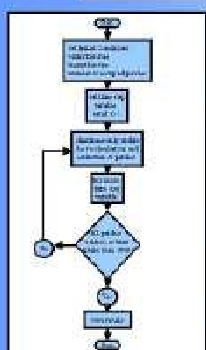

ASSUMPTIONS AND LIMITATIONS

THE ISSUE

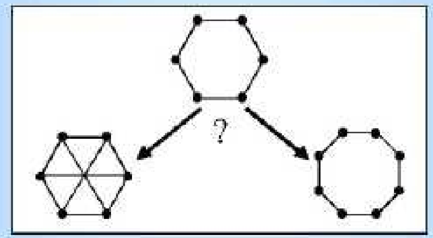

A metapopulation is a collection of discrete population patches, in which individual patches may typically go extinct and be recolonized. Is the long-term viability of the metapopulation helped more by adding new patches or by increasing the number of migration pathways between existing patches?

Adding patches increases the overall population of the organism, and makes a total extinction less likely by increasing the direct number of patches which would have to go extinct.

Adding migration pathways increases the likelihood of recolonization of extinct patches, by giving extinct patches more sources for immigration.

RESULTS

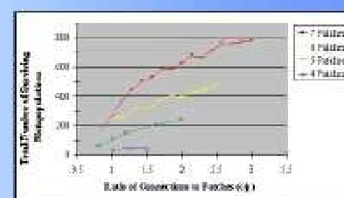

CONCLUSIONS

Fusing [18]FDG-hybrid PET To CT Images Significantly Alters Treatment Planning In The Radical Treatment Of Non-Small Cell Lung Carcinoma

Y.C. Ung, M.D., C.B. Caldwell, Ph.D.,[1] K. Mah, M.Sc., C.E. Danjoux, M.D., J.M. Balogh, M.D., S.N. Ganguli, M.D.,[1] R.G. Tirona, B.Sc., and L.E. Ehrlich, M.D.[1]
Toronto-Sunnybrook Regional Cancer Centre, Sunnybrook and Women's College Health Sciences Centre,[1] and University of Toronto, Toronto, CANADA

Abstract

Problem

Potential of [18]FDG-hybrid PET for Radiation Therapy Planning

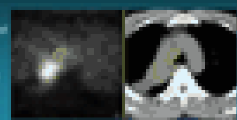

Study Objective: To determine the impact of integrating [18]FDG-hybrid PET images with CT planning images on treatment planning of patients with NSCLC.

Prospective Study Design

Imaging: in treatment position and same day

FDG-hybrid PET

CT simulation

Image Registration

Patient Selection

Treatment Planning

Impact of FDG-hybrid PET on Patient Management

- In 5/26 (19%) patients, radiation therapy was changed from radical to palliative intent.

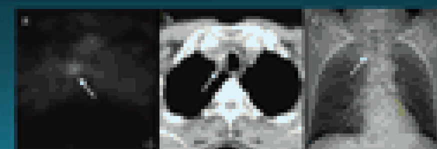

Impact of Co-registered FDG-hybrid PET on PTV Coverage

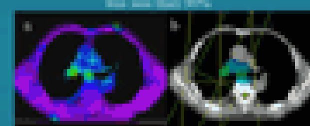

Impact of FDG-hybrid PET on Spinal Cord Dose

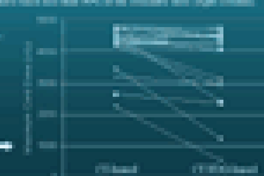

Discussion

Conclusions

LESSONS LEARNED FROM AIRWAY PRESSURE RELEASE VENTILATION (APRV)

Lewis J. Kaplan, MD[1][2], Heatherlee Bailey, MD, FAAEM[2]
Medical College of Pennsylvania-Hahnemann University
Departments of Surgery[1] and Emergency Medicine[2], Philadelphia, PA USA

INTRODUCTION

Airway Pressure Release Ventilation (APRV, a.k.a. BIPAP) has been previously demonstrated to be a useful modality to manage patients with acute lung injury (ALI) or the acute respiratory distress syndrome (ARDS). As this is a fundamentally different mode than conventional cyclic ventilation, we reviewed a single institution's experience with APRV to determine safety, complication detection, and efficacy at resolving hypoxemia and hypercarbia.

METHODS

Consecutive patients transitioned from either volume or pressure targeted ventilation to APRV (Dräger Evita 4 Pulmonary Workstation) at a University hospital surgical ICU were retrospectively reviewed. Patients initially ventilated with APRV were excluded. Initial ARPV settings to correct hypoxemia ($pO_2 \leq 60$ torr on $FIO_2 \geq 0.9$) were a P_{High} at the prior plateau pressure, a T_{High} of 6.0 sec and a T_{Low} of 0.8 sec. Hypercarbic ($pCO_2 \geq 55$ torr and $pH \leq 7.2$) patients were set to a T_{High} of 5.0 sec and a T_{Low} of 1.0 sec. Settings were adjusted to resolve hypoxemia and hypercarbia. IRB approved abstracted data included principal diagnoses, ventilation parameters, laboratory values and ventilator associated complications. Data before and after APRV were compared using a two-tailed paired t-test or Chi-square as appropriate; significance was assumed for $p < 0.05$ ([5]).

RESULTS

Demographics

APRV

Element	Value
% Hypoxemia	88%
% Hypercarbia	12%
Time to $S_pO_2 \geq 92\%$	7 ± 4 min
Time to $FIO_2 \leq 0.6$	5.2 ± 0.9 hr
Time to pt $O_2 \leq 40$ torr	42 ± 7 min
Time to max Δ pCO_2	76 ± 12 min
Mean change in V_T	-5.3 ± 0.9 L/min[6]

Transport Safety

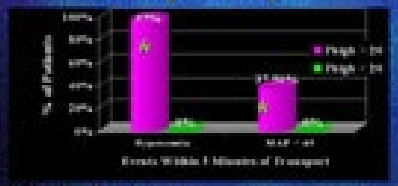

Complications

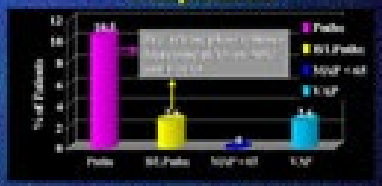

CONCLUSIONS

1. APRV is a safe rescue mode for hypoxemic or hypercarbic respiratory failure and requires a significantly lower V_T than conventional ventilation.
2. Decreasing release phase volumes and a rising pCO_2 are strong indicators of pneumothorax in a patient on APRV. Routine end-tidal CO_2 monitoring is recommended.
3. Preparation for safe intra-hospital transport may be keyed to the P_{high} required for oxygenation and ventilation. Patients requiring a $P_{high} > 20$ cm H_2O should be transported on the ventilator.